Secure Intelligent Reflecting Surface-Aided Integrated Sensing and Communication

Meng Hua, *Member, IEEE*, Qingqing Wu, *Senior Member, IEEE*, Wen Chen, *Senior Member, IEEE*, Octavia A. Dobre, *Fellow, IEEE*, and A. Lee Swindlehurst, *Fellow, IEEE*

***Abstract*— In this paper, an intelligent reflecting surface (IRS) is leveraged to enhance the physical layer security of an integrated sensing and communication (ISAC) system in which the IRS is deployed to not only assist the downlink communication for multiple users, but also create a virtual line-of-sight (LoS) link for target sensing. In particular, we consider a challenging scenario where the target may be a suspicious eavesdropper that potentially intercepts the communication-user information transmitted by the base station (BS). To ensure the sensing quality while preventing the eavesdropping, dedicated sensing signals are transmitted by the BS. We investigate the joint design of the phase shifts at the IRS and the communication as well as radar beamformers at the BS to maximize the sensing beampattern gain towards the target, subject to the maximum information leakage to the eavesdropping target and the minimum signal-to-interference-plus-noise ratio (SINR) required by users. Based on the availability of perfect channel state information (CSI) of all involved user links and the potential target location of interest at the BS, two scenarios are considered and two different optimization algorithms are proposed. For the ideal scenario where the CSI of the user links and the potential target location are perfectly known at the BS, a penalty-based algorithm is proposed to obtain a high-quality solution. In particular, the beamformers are obtained with a semi-closed-form solution using Lagrange duality and the IRS phase shifts are solved for in closed form by applying the majorization-minimization (MM) method. On the other hand, for the more practical scenario where the CSI is imperfect and the potential target location is uncertain in a region of interest, a robust algorithm based on the $\mathcal{S}$-procedure and sign-definiteness approaches is proposed. Simulation results demonstrate the effectiveness of the proposed scheme in achieving a trade-off between the communication quality and the sensing quality, and also show the tremendous potential of IRS for use in sensing and improving the security of ISAC systems.**

***Index Terms*— Intelligent reflecting surface, integrated sensing and communication, physical layer security.**

Manuscript received 5 September 2022; revised 17 February 2023 and 4 May 2023; accepted 19 May 2023. Date of publication 2 June 2023; date of current version 9 January 2024. The work of Wen Chen was supported in part by the National Key Project under Grant 2020YFB1807700; in part by NSFC under Grant 62071296; and in part by Shanghai under Grant 22JC1404000, Grant 20JC1416502, and Grant PKX2021-D02. The work of Octavia A. Dobre was supported in part by the Natural Sciences and Engineering Research Council of Canada (NSERC) through its Discovery Program. The work of A. Lee Swindlehurst was supported by the U.S. National Science Foundation under Grant ECCS-2030029 and Grant CNS-2107182. The associate editor coordinating the review of this article and approving it for publication was Z. Zhang. *(Corresponding author: Qingqing Wu.)*

Meng Hua is with the Department of Electronic Engineering, Shanghai Jiao Tong University, Shanghai 200240, China, and also with the State Key Laboratory of Internet of Things for Smart City, University of Macau, Macau, China (e-mail: menghua@um.edu.mo).

Qingqing Wu is with the Department of Electronic Engineering, Shanghai Jiao Tong University, Shanghai 200240, China (e-mail: qingqingwu@sjtu.edu.cn).

Wen Chen is with the Department of Electronic Engineering, Shanghai Institute of Advanced Communications and Data Sciences, Shanghai Jiao Tong University, Shanghai 200240, China (e-mail: wenchen@sjtu.edu.cn).

Octavia A. Dobre is with the Faculty of Engineering and Applied Science, Memorial University, St. John's, NL A1B 3X5, Canada (e-mail: odobre@mun.ca).

A. Lee Swindlehurst is with the Center for Pervasive Communications and Computing, University of California at Irvine, Irvine, CA 92697 USA (e-mail: swindle@uci.edu).

Color versions of one or more figures in this article are available at https://doi.org/10.1109/TWC.2023.3280179.

Digital Object Identifier 10.1109/TWC.2023.3280179

I. Introduction

DRIVEN by emerging applications for high-accuracy sensing services such as autonomous driving, robot navigation, and intelligent traffic monitoring, etc., a new paradigm is required to shift from communication-based network designs to networks with sensing-communication integration [1]. The research on the integration of sensing and communication networks has recently attracted significant attention along the following two directions: radar-communication coexistence [2] and integrated sensing and communication (ISAC) [3]. In the former, the radar transceiver and the communication transmitter are geographically separated, which usually results in strong co-channel interference and requires prohibitive feedback overhead to exchange information for coordination between two systems. For the latter, the radar and communication functionalities share a common hardware platform, which leads to both integration and coordination gains.

Recently, we are witnessing a booming interest from both academia and industry on ISAC systems due to the additional integration gain and coordination gain brought compared to the radar-communication coexistence systems [4], [5]. Based on design priorities and underlying requirements, ISAC systems can be classified into three categories: communication-centric (C&C) designs [6], radar-centric (R&C) designs [7], and joint waveform designs [8], [9], [10]. For C&C design, the sensing functionality is integrated into the existing communication platform, where the communication performance has the highest priority. The objective of this type of design is to exploit the communication waveform to implement the sensing functionality while satisfying the quality-of-service (QoS) of the communication users. In contrast to the C&C design, sensing has the highest priority in R&C designs. The objective of this approach is to modulate the information into

the sensing waveform to realize the communication functionality without significantly degrading the sensing performance. The performance of the two types of designs above is fundamentally limited by the hardware platforms and signal processing algorithms and fails to achieve a scalable tradeoff between sensing and communication. The last category, i.e., joint waveform design, creates new waveforms instead of relying on existing communication or radar waveforms, and provides additional degrees of freedom (DoFs) to support high data rates and to improve sensing quality. As an example of the joint design approach, the authors in [8] revealed that communication-only waveform design is inferior to the joint design of communication and radar waveforms in terms of beampattern synthesis, especially when the number of communication users is less than the number of targets. However, the ISAC system performance is significantly deteriorated by unfavorable propagation environments with signal blockages, especially for target sensing. In general, only the reflected echo signals that pass through line-of-sight (LoS) links are treated as useful information for sensing while non-LoS (NLoS) links are treated as harmful interference or clutter. Unmanned aerial vehicles (UAVs) have been leveraged to assist ISAC systems since the UAV can establish strong LoS links between the UAV and users/targets by adjusting its trajectory or deployment [11], [12], [13], [14]. However, the UAV-enabled ISAC is not suitable for providing long-term coverage due to the inherently limited battery capacity available on a UAV. This raises a new open question: How to provide long-term and ubiquitous sensing coverage in harsh environments where the channel links are blocked in the ISAC system?

Recently, intelligent reflecting surface (IRS) technology has attracted significant attention and is regarded as a promising technology towards for beyond-fifth-generation (B5G) and sixth-generation (6G) systems, due to its capability of manipulating the wireless propagation environment with low power consumption and hardware cost [15], [16]. Specifically, an IRS is a two-dimensional planar array comprising a large number of sub-wavelength metallic units, each of which is able to independently control the phases and/or amplitudes of impinging signals. Due to the small size of each reflecting unit, a reasonably-sized IRS can be constructed with a large number of reflecting elements and can provide significant beamforming gains to compensate for signal attenuation over long distances [17]. Motivated by this, IRS technology has been extensively investigated in the literature for various applications such as mobile edge computing (MEC) [18], [19], [20], wireless power transfer [21], [22], [23], [24], and multi-cell cooperation [25], [26], [27]. The use of IRS is very appealing for ISAC [28]. Specifically, the IRS is able to create virtual LoS links for both communication and sensing as well as introduce additional degrees of freedom for optimization. By carefully deploying IRS and adjusting its phase shifts, the IRS can boost the desired target returns and suppress interference by manipulating the propagation environment. Therefore, the IRS will not only enhances the sensing performance for targets that already enjoys LoS propagation, but also allows the radar to sense targets in shadowed areas that would normally be invisible to the radar. Some representative works, see e.g., [29], [30], [31], have studied the use of IRS for sensing and verified their potential for enhancing target sensing. A handful of related works have been conducted on IRS-aided ISAC in the literature, see [32], [33], [34], [35], and [36], via jointly optimizing IRS phase shifts and transmit beamformers to increase the sensing quality while satisfying communication QoS of the users. However, the above works assume that the targets are not attempting to intercept the transmitted signals. In ISAC systems, the transmitted signals may not only contain sensing signals but also communication signals, and these signals could be readily intercepted by malicious targets. The problem of maintaining the communication QoS and the target sensing performance while also ensuring that information is not leaked to the targets has received very little attention. Although works [37], [38] studied secure transmission designs for ISAC system, the role of IRS for sensing and communication was not unveiled and the previous transceiver design was also no longer applicable.

Motivated by the above issues, in this paper we study a secure IRS-aided ISAC system where the IRS is leveraged to not only assist the downlink communication from the base station (BS) to multiple legitimate users, but to also create a virtual LoS link for target sensing. In addition, we consider a challenging scenario where the target may be an eavesdropper that desires to intercept information transmitted by the BS. The main contributions of this paper are summarized as follows:

- We study an IRS-aided ISAC system for enhancing the physical layer security and realizing both communication and sensing. To ensure the sensing quality while preventing eavesdropping, dedicated sensing signals are transmitted at the BS. Our objective is to maximize the sensing beampattern gain by jointly optimizing the communication beamformers, radar beamformers, and IRS phase shifts, subject to the maximum tolerable information leakage to the eavesdropping target and the minimum signal-to-interference-plus-noise ratio (SINR) required by the users. Based on whether or not perfect channel state information (CSI) and potential target location of interest are known by BS, two different optimization problems are formulated. Subsequently, two different algorithms are proposed, i.e., a penalty-based algorithm and a robust algorithm.
- For the ideal scenario where the CSI of the user links and the potential target location of interest are known at the BS, the resulting optimization problem is non-convex due to the presence of coupled optimization variables in both the objective function and constraints. In addition, the unit-modulus constraint imposed on each IRS phase shift renders the formulated problem more difficult to solve. To address this difficulty, a penalty-based algorithm is proposed in which the beamformers are obtained with a semi-closed-form solution using Lagrange duality and the IRS phase shifts are obtained with a closed-form solution by applying majorization-minimization (MM), both of which significantly reduce the computational complexity of the penalty-based algorithm.
- For the more practical scenario where perfect CSI of communication channels and the potential target location

in a region of interest are not known at the BS, we design a robust transmission strategy. The resulting optimization problem involving an infinite number of constraints is more challenging to solve than the former one, and the previous penalty-based algorithm is no longer applicable. To solve this optimization problem, the $\mathcal{S}$-procedure and sign-definiteness approaches are applied to transform the infinite number of inequalities into a finite number of linear matrix inequalities (LMIs). Then, an efficient alternating optimization (AO) algorithm is proposed that toggles between optimizing the transmit beamformers and IRS phase shifts.

- Our simulation results verify the effectiveness of the proposed scheme in achieving a flexible trade-off between the communication quality and the target sensing quality and validate the tremendous potential of IRS to achieve significant beampattern gains and guarantee ISAC system security. Our results also show that dedicated sensing signals are required to further improve the system performance.

The rest of the paper is organized as follows. Section II introduces the system model and problem formulations for the considered IRS-aided secure ISAC system. In Section III, a penalty-based algorithm is proposed to solve the perfect CSI and the known-target location case. In Section IV, a robust design algorithm is proposed to solve the case with imperfect CSI and uncertain target location. Numerical results are provided in Section V and the paper is concluded in Section VI.

Notations: Boldface upper-case and lower-case letters denote matrices and vectors, respectively. $\mathbb{C}^{d_1\times d_2}$ stands for the set of complex $d_1 \times d_2$ matrices. For a complex-valued vector $\mathbf{x}$, $\|\mathbf{x}\|$ represents the Euclidean norm of $\mathbf{x}$, $\arg(\mathbf{x})$ denotes a vector containing the phase of the elements of $\mathbf{x}$, and $\mathrm{diag}(\mathbf{x})$ denotes a diagonal matrix whose diagonal elements are given by the elements of $\mathbf{x}$. $(\cdot)^T, (\cdot)^*$, and $(\cdot)^H$ stand for the transpose operator, conjugate operator, and conjugate transpose operator, respectively. $\|\mathbf{X}\|_F$ and $\mathrm{rank}\,(\mathbf{X})$ represent the Frobenius norm and rank of $\mathbf{X}$, respectively, and $\mathbf{X} \succeq \mathbf{0}$ indicates that matrix $\mathbf{X}$ is positive semi-definite. A circularly symmetric complex Gaussian random variable x with mean μ and variance σ^2 is denoted by $x \sim \mathcal{CN}\left(\mu, \sigma^2\right)$. $\otimes$ denotes the Kronecker product operator and $\mathcal{O}\left(\cdot\right)$ indicates the big-O computational complexity.

II. System Model and Problem Formulation

A. System Model

We consider a secure IRS-aided ISAC system that comprises a dual-function BS, an IRS,[1] one target of interest,[2] and K single-antenna users, as shown in Fig. 1. The BS is equipped with a uniform linear array with N transmit antennas ($N \geq K$), and the IRS is a uniform planar array with M reflecting elements. For convenience, we denote the sets of users, BS transmit antennas, and IRS reflecting elements as $\mathcal{K}$, $\mathcal{N}$, and $\mathcal{M}$, respectively. The transmission protocol for the IRS-aided ISAC system can be described by following steps: 1) the downlink (DL) channel state information (CSI) of communication links can be obtained at the BS via sending the pilot signals by users (We assume that the uplink (UL) and DL channels are reciprocal so that the DL CSI can be obtained via the UL channel estimation) [39]. In addition, the target information can be obtained via analyzing the echo signals reflected by the target [40] or we can assume that the target is located in the certain region we are interested in. 2) The resource allocation and IRS phase shifts are computed at the BS by applying the proposed algorithms in this paper. 3) The BS sends the optimized phase shifts to the IRS controller to adjust the IRS phase shifts, and then the BS and the IRS start to transmit signals to communicate users and sense target.

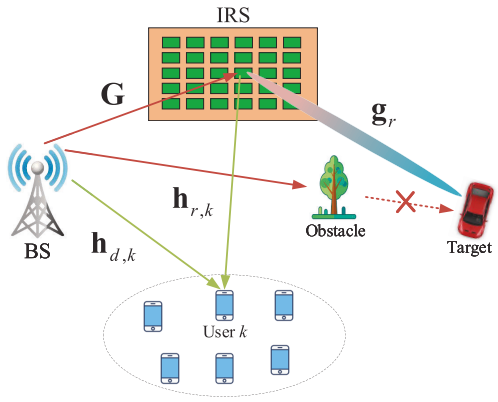

Fig. 1. An IRS-aided secure ISAC system.

We assume that both information signals and radar signals are simultaneously transmitted for communication and sensing by the shared antennas.[3] As such, the transmitted signals at the BS can be expressed as

$$\mathbf{s} = \sum_{k=1}^{K} \mathbf{w}_{c,k} x_{c,k} + \sum_{n=1}^{N} \mathbf{w}_{r,n} x_{r,n}, \tag{1}$$

where $x_{c,k}$ denotes the information signal for user k assumed to satisfy $x_{c,k} \sim \mathcal{CN}(0,1)$ and $\mathbf{w}_{c,k} \in \mathbb{C}^{N\times 1}$ represents its corresponding communication beamformer. Similarly, $x_{r,n}$ denotes the nth radar signal satisfying $\mathbb{E}\{x_{r,n}\} = 0$ and $\mathbb{E}\left\{|x_{r,n}|^2\right\} = 1$, and $\mathbf{w}_{r,n} \in \mathbb{C}^{N\times 1}$ represents the corresponding radar beamformer. We assume that communication and radar signals are statistically independent and uncorrelated, i.e., $\mathbb{E}\left\{x_{r,n} x_{c,k}^H\right\} = 0, \forall k, n$.

1) Communication Model: We consider quasi-static block-fading channels and focus on a given fading block during which all the channels involved are assumed to remain unchanged. Let $\mathbf{G} \in \mathbb{C}^{M\times N}$ denote the complex equivalent

[1]Although the system considers a single IRS, the algorithms proposed for the single-IRS case are applicable to the multi-IRS case without any modifications.

[2]Although we consider a single target in this paper, our problem can be readily extended to the case with multiple targets. In addition, our proposed algorithm is also applicable to the multiple targets case with slight modifications.

[3]The shared antenna deployment strategy is superior than the separated antenna deployment strategy in terms of sensing quality and communication quality [41].

baseband channel from the BS to the IRS, $\mathbf{h}_{r,k}^H \in \mathbb{C}^{1\times M}$ denote that from the IRS to user k, and $\mathbf{h}_{d,k}^H \in \mathbb{C}^{1\times N}$ denote that from the BS to user k, $k \in \mathcal{K}$. We assume that the CSI of all involved channels, i.e., $\mathbf{G}$, $\mathrm{diag}\left(\mathbf{h}_{r,k}^H\right)\mathbf{G}$, and $\mathbf{h}_{d,k}^H$, is available at the BS by applying the state-of-the-art two-timescale channel estimation method [42]. Note that the CSI of the BS-IRS link, i.e., $\mathbf{G}$, is required in this paper for target sensing, which will be shown later. The signal received at user k is given by

$$y_k = \left(\mathbf{h}_{r,k}^H \boldsymbol{\Theta} \boldsymbol{G} + \mathbf{h}_{d,k}^H\right)\mathbf{s} + n_k, k \in \mathcal{K}, \tag{2}$$

where $\boldsymbol{\Theta} = \mathrm{diag}\left(v_1, \ldots, v_M\right)$ represents the IRS reflection phase shift matrix and $n_k \sim \mathcal{CN}\left(0, \sigma_k^2\right)$ denotes the noise received at user k. Accordingly, the received SINR at user k is given by

$$\gamma_k = \frac{\left|\mathbf{h}_k^H \mathbf{w}_{c,k}\right|^2}{\sum\limits_{i\neq k}^{K}\left|\mathbf{h}_k^H \mathbf{w}_{c,i}\right|^2 + \sum\limits_{n=1}^{N}\left|\mathbf{h}_k^H \mathbf{w}_{r,n}\right|^2 + \sigma_k^2}, \quad k \in \mathcal{K}, \tag{3}$$

where $\mathbf{h}_k^H = \mathbf{h}_{r,k}^H \boldsymbol{\Theta} \boldsymbol{G} + \mathbf{h}_{d,k}^H$.

2) Radar Sensing and Interception Model: We consider the scenario where the direct link between the BS and the potential target location is not available due to the blockages. To tackle this issue, the IRS is leveraged to create a virtual LoS link between the IRS and the target, thereby establishing an effective BS-IRS-target link for sensing. Let θ and φ denote the azimuth and elevation angle-of-departure (AoD) from the IRS to the target, respectively. Accordingly, the steering vector from the IRS to the target at direction (θ, φ) can be expressed as

$$\begin{aligned}\mathbf{g}_r^H = \alpha_r &\left[1, e^{-j\frac{2\pi d}{\lambda}\sin\theta\cos\varphi}, \ldots e^{-j\frac{2\pi(M_x-1)d}{\lambda}\sin\theta\cos\varphi}\right] \\ &\otimes \left[1, e^{-j\frac{2\pi d}{\lambda}\sin\theta\sin\varphi}, \ldots e^{-j\frac{2\pi(M_z-1)d}{\lambda}\sin\theta\sin\varphi}\right],\end{aligned} \tag{4}$$

where M_x and M_z denote the numbers of reflecting elements along x-axis and z-axis, respectively, α_r represents the large-scale fading coefficient, λ denotes the wavelength, and d denotes the spacing between two adjacent reflecting elements. The received signal at the target is given by

$$y_t = \mathbf{g}_r^H \boldsymbol{\Theta} \boldsymbol{G}\left(\sum_{k=1}^{K}\mathbf{w}_{c,k}x_{c,k} + \sum_{n=1}^{N}\mathbf{w}_{r,n}x_{r,n}\right) + n_t, \tag{5}$$

where $n_t \sim \mathcal{CN}\left(0, \sigma_t^2\right)$ represents the noise received at the target. As a result, the beampattern gain towards the target is given by

$$\begin{aligned}\mathcal{P} &= \mathbb{E}\left\{\left|\mathbf{g}^H\left(\sum_{k=1}^{K}\mathbf{w}_{c,k}x_{c,k} + \sum_{n=1}^{N}\mathbf{w}_{r,n}x_{r,n}\right)\right|^2\right\} \\ &= \mathbf{g}^H\left(\sum_{k=1}^{K}\mathbf{w}_{c,k}\mathbf{w}_{c,k}^H + \sum_{n=1}^{N}\mathbf{w}_{r,n}\mathbf{w}_{r,n}^H\right)\mathbf{g},\end{aligned} \tag{6}$$

where $\mathbf{g}^H = \mathbf{g}_r^H \boldsymbol{\Theta} \boldsymbol{G}$.

Since the target is a potential eavesdropper, it tries to decode information from its received signals. The SINR received at the target for intercepting user k's information is given by[4]

$$\gamma_{e,k} = \frac{\left|\mathbf{g}^H \mathbf{w}_{c,k}\right|^2}{\sum\limits_{i\neq k}^{K}\left|\mathbf{g}^H \mathbf{w}_{c,i}\right|^2 + \sum\limits_{n=1}^{N}\left|\mathbf{g}^H \mathbf{w}_{r,n}\right|^2 + \sigma_t^2}, \quad k \in \mathcal{K}. \tag{7}$$

B. Problem Formulation

The objective of this paper is to maximize the beampattern gain at the target by jointly optimizing the transmit beamformers and IRS phase shifts, subject to the minimum SINR required by users and the maximum tolerable information leakage to the target. Depending on whether perfect CSI of the communication channels and the target location are available at the BS, we consider two scenarios elaborated as below.

1) Perfect CSI and Known Target Location Scenario: In this scenario, perfect CSI of the communication channels and the potential target location of interest are known at the BS. Accordingly, the problem is formulated as

$$\max_{\{\mathbf{w}_{c,k}, \mathbf{w}_{r,n}, v_m\}} \mathbf{g}^H\left(\sum_{k=1}^{K}\mathbf{w}_{c,k}\mathbf{w}_{c,k}^H + \sum_{n=1}^{N}\mathbf{w}_{r,n}\mathbf{w}_{r,n}^H\right)\mathbf{g} \tag{8a}$$

$$\text{s.t. } \gamma_k \geq r_{k,\mathrm{th}}, \quad k \in \mathcal{K}, \tag{8b}$$

$$\gamma_{e,k} \leq r_{e,k,\mathrm{th}}, \quad k \in \mathcal{K}, \tag{8c}$$

$$\sum_{k=1}^{K}\left\|\mathbf{w}_{c,k}\right\|^2 + \sum_{n=1}^{N}\left\|\mathbf{w}_{r,n}\right\|^2 \leq P_{\max}, \tag{8d}$$

$$|v_m| = 1, \quad m \in \mathcal{M}, \tag{8e}$$

where $r_{k,\mathrm{th}}$ in (8b) denotes the minimum SINR required by user k, $r_{e,k,\mathrm{th}}$ in (8c) represents the maximum tolerable leakage of user k's information to the target, $P_{\max}$ in (8d) stands for the maximum allowed transmit power at the BS, and constraint (8e) denotes the unit-modulus constraint imposed on each IRS phase shift. Note that with constraints (8b) and (8c), the level of physical layer security of the ISAC system is guaranteed [43], such that the system secrecy rate of user k is bounded by $\log_2\left(1 + r_{k,\mathrm{th}}\right) - \log_2\left(1 + r_{e,k,\mathrm{th}}\right)$.

2) Imperfect CSI and Uncertain Target Location Scenario: In this scenario, perfect CSI of the communication channels is not available at the BS, and the potential target location in a region of interest is unknown, i.e., $\Phi_h = [\theta - \Delta\theta, \theta + \Delta\theta]$ and $\Phi_v = [\varphi - \Delta\varphi, \varphi + \Delta\varphi]$ are known, where $\Delta\theta$ and $\Delta\varphi$ represent the azimuth and vertical sensing range, respectively. Defining $\mathbf{F}_k = \mathrm{diag}\left(\mathbf{h}_{r,k}^H\right)\mathbf{G}$ and $\mathbf{F}_r = \mathrm{diag}\left(\mathbf{g}_r^H\right)\mathbf{G}$, we can rewrite $\mathbf{h}_k^H = \mathbf{h}_{r,k}^H \boldsymbol{\Theta} \boldsymbol{G} + \mathbf{h}_{d,k}^H = \mathbf{v}^H \mathbf{F}_k + \mathbf{h}_{d,k}^H$ and $\mathbf{g}^H = \mathbf{g}_r^H \boldsymbol{\Theta} \boldsymbol{G} = \mathbf{v}^H \mathbf{F}_r$, where $\mathbf{v}^H = [v_1, \ldots, v_M]$. The bounded CSI error models for channels $\mathbf{F}_k$, $\mathbf{F}_r$, and $\mathbf{h}_{d,k}$ are respectively given by [44][5]

$$\mathbf{F}_k = \hat{\mathbf{F}}_k + \Delta\mathbf{F}_k, \text{ with } \mathcal{F}_k = \left\{\Delta\mathbf{F}_k : \left\|\Delta\mathbf{F}_k\right\|_F \leq \varepsilon_k\right\}, \tag{9}$$

[4]If the true target locates elsewhere, we can directly impose the physical layer security constraint on it if we know its location and increase the sensing region to cover the potential target if the location of the true target is unknown.

[5]The bounded CSI error models for $\mathbf{F}_r$ and $\mathbf{G}$ are equivalent since $\mathbf{g}_r^H$ is a deterministic LoS channel. For notational simplicity, we use the bounded CSI error model for $\mathbf{F}_r$ in the sequel.

$$\mathbf{F}_r = \hat{\mathbf{F}}_r + \Delta\mathbf{F}_r, \text{ with } \mathcal{F}_r = \left\{\Delta\mathbf{F}_r : \|\Delta\mathbf{F}_r\|_F \le \varepsilon_r\right\}, \tag{10}$$

$$\mathbf{h}_{d,k} = \hat{\mathbf{h}}_{d,k} + \Delta\mathbf{h}_{d,k}, \text{ with } \mathcal{H}_{d,k} = \left\{\Delta\mathbf{h}_{d,k} : \|\Delta\mathbf{h}_{d,k}\| \le \varepsilon_{d,k}\right\}, k \in \mathcal{K}, \tag{11}$$

where $\hat{\mathbf{G}}$ represents the estimated channel for the BS-IRS link, $\hat{\mathbf{F}}_k$ denotes the estimated cascaded channel for user k, $\hat{\mathbf{F}}_r = \text{diag}\left(\mathbf{g}_r^H\right)\hat{\mathbf{G}}$ stands for the estimated cascaded channel for the target. Accordingly, the problem is formulated as[6]

$$\max_{\{\mathbf{w}_{c,k},\mathbf{w}_{r,n},v_m\}} \min_{\substack{\theta_h\in\Phi_h,\\ \varphi_v\in\Phi_v}} \mathbf{g}^H\left(\sum_{k=1}^K \mathbf{w}_{c,k}\mathbf{w}_{c,k}^H + \sum_{n=1}^N \mathbf{w}_{r,n}\mathbf{w}_{r,n}^H\right)\mathbf{g} \tag{12a}$$

$$\text{s.t. } \gamma_k \ge r_{k,\text{th}}, \quad \Delta\mathbf{h}_{d,k} \in \mathcal{H}_{d,k}, \ \Delta\mathbf{F}_k \in \mathcal{F}_k, \ k \in \mathcal{K}, \tag{12b}$$

$$\gamma_{e,k} \le r_{e,k,\text{th}}, \quad \theta_h \in \Phi_h, \quad \varphi_v \in \Phi_v, \quad \Delta\mathbf{F}_r \in \mathcal{F}_r, \ k \in \mathcal{K}, \tag{12c}$$

$$\sum_{k=1}^K \|\mathbf{w}_{c,k}\|^2 + \sum_{n=1}^N \|\mathbf{w}_{r,n}\|^2 \le P_{\max}, \tag{12d}$$

$$|v_m| = 1, \quad m \in \mathcal{M}. \tag{12e}$$

The above two problems (8) and (12) are both non-convex due to the fact that the IRS reflection coefficients are constrained to be unit modulus, and because the optimization variables are coupled in both the objective functions and constraints. In general, there are no standard methods for solving such non-convex optimization problems optimally. In particular, (12b) and (12c) involve an infinite number of inequalities, which makes problem (12) even more difficult to address. In the following, we first propose a penalty-based algorithm for solving problem (8) in Section III and then propose an AO algorithm based on the $\mathcal{S}$-procedure and sign-definiteness approaches for solving problem (12) in Section IV.

III. Proposed Solution for Perfect CSI and Known Target Location

In this section, we consider the case where perfect CSI and the potential target location of interest are known at the BS, which provides a performance upper bound for the case with imperfect CSI and uncertain target location. To obtain a high-quality solution for problem (8), a penalty-based algorithm is proposed to decouple constraint coupling between the optimization variables in different blocks. Define auxiliary variables $\{y_{c,k}, y_{r,n}, z_{c,k,i}, z_{r,k,n}, i \in \mathcal{K}, k \in \mathcal{K}, n \in \mathcal{N}\}$ and let $\mathbf{g}^H\mathbf{w}_{c,k} = y_{c,k}$, $\mathbf{g}^H\mathbf{w}_{r,n} = y_{r,n}$, $\mathbf{h}_k^H\mathbf{w}_{c,i} = z_{c,k,i}$, and $\mathbf{h}_k^H\mathbf{w}_{r,n} = z_{r,k,n}$. Problem (8) can be equivalently transformed as

$$\max_{\{\mathbf{w}_{c,k}\},\{\mathbf{w}_{r,n}\},\{v_m\},\Omega} \sum_{k=1}^K |y_{c,k}|^2 + \sum_{n=1}^N |y_{r,n}|^2 \tag{13a}$$

$$\text{s.t. } \frac{|z_{c,k,k}|^2}{\sum_{i\ne k}^K |z_{c,k,i}|^2 + \sum_{n=1}^N |z_{r,k,n}|^2 + \sigma_k^2} \ge r_{k,\text{th}}, \quad k \in \mathcal{K}, \tag{13b}$$

$$\frac{|y_{c,k}|^2}{\sum_{i\ne k}^K |y_{c,i}|^2 + \sum_{n=1}^N |y_{r,n}|^2 + \sigma_t^2} \le r_{e,k,\text{th}}, \quad k \in \mathcal{K}, \tag{13c}$$

$$\mathbf{g}^H\mathbf{w}_{c,k} = y_{c,k}, \quad \mathbf{g}^H\mathbf{w}_{r,n} = y_{r,n}, \quad \mathbf{h}_k^H\mathbf{w}_{c,k} = z_{c,k,i}, \quad \mathbf{h}_k^H\mathbf{w}_{r,n} = z_{r,k,n}, \quad i \in \mathcal{K}, \ k \in \mathcal{K}, \ n \in \mathcal{N}, \tag{13d}$$

$$\text{(8d), (8e)}, \tag{13e}$$

where $\Omega = \{y_{c,k}, y_{r,n}, z_{c,k,i}, z_{r,k,n}\}$. We then reformulate (13d) as penalty terms that are added to the objective function (13a) yielding the following optimization problem

$$\begin{aligned}\max_{\{\mathbf{w}_{c,k},\mathbf{w}_{r,n},v_m\},\Omega} & \sum_{k=1}^K |y_{c,k}|^2 + \sum_{n=1}^N |y_{r,n}|^2 - \frac{1}{2\rho} \\ & \times \left(\sum_{k=1}^K \left|\mathbf{g}^H\mathbf{w}_{c,k} - y_{c,k}\right|^2 + \sum_{n=1}^N \left|\mathbf{g}^H\mathbf{w}_{r,n} - y_{r,n}\right|^2 \right. \\ & + \sum_{k=1}^K\sum_{i=1}^K \left|\mathbf{h}_k^H\mathbf{w}_{c,i} - z_{c,k,i}\right|^2 \\ & \left. + \sum_{k=1}^K\sum_{n=1}^N \left|\mathbf{h}_k^H\mathbf{w}_{r,n} - z_{r,k,n}\right|^2\right)\end{aligned} \tag{14a}$$

$$\text{s.t. (8d), (8e), (13b), (13c)}, \tag{14b}$$

where $\rho > 0$ represents the parameter that penalizes the violations of the equality constraints in (13d). To address problem (14), a penalty-based algorithm comprising two layers is proposed, where in the outer layer, we gradually update the penalty parameter, while in the inner loop, we alternately optimize the variables in different blocks.

A. Inner Layer Optimization

In the inner layer, we divide all the optimization variables into three blocks: 1) auxiliary variable set Ω, 2) transmit beamformers $\{\mathbf{w}_{c,k}, \mathbf{w}_{r,n}\}$, and 3) IRS phase shifts $\{v_m\}$.

1) Optimizing Ω for Given $\{\mathbf{w}_{c,k}, \mathbf{w}_{r,n}\}$ and $\{v_m\}$: This subproblem can be written as

$$\begin{aligned}\max_{\Omega} & \sum_{k=1}^K |y_{c,k}|^2 + \sum_{n=1}^N |y_{r,n}|^2 - \frac{1}{2\rho} \\ & \times \left(\sum_{k=1}^K \left|\mathbf{g}^H\mathbf{w}_{c,k} - y_{c,k}\right|^2 + \sum_{n=1}^N \left|\mathbf{g}^H\mathbf{w}_{r,n} - y_{r,n}\right|^2 \right. \\ & \left. + \sum_{k=1}^K\sum_{i=1}^K \left|\mathbf{h}_k^H\mathbf{w}_{c,i} - z_{c,k,i}\right|^2 + \sum_{k=1}^K\sum_{n=1}^N \left|\mathbf{h}_k^H\mathbf{w}_{r,n} - z_{r,k,n}\right|^2\right)\end{aligned} \tag{15a}$$

$$\text{s.t. (13b), (13c)}. \tag{15b}$$

Since the optimization variables with respect to (w.r.t.) different blocks $\{y_{c,k}, y_{r,n}, \forall k, \forall n\}$ and $\{z_{c,k,i}, z_{r,k,n}, \forall i, \forall n\}$ for $k \in \mathcal{K}$ are separable in both the objective function and constraints, we can independently solve $K+1$ subproblems in parallel. Specifically, the subproblem corresponding to the

[6]In this scenario, we drop the direction indices, i.e., θ_h and φ_v, and use the notation $\mathbf{g}$ to represent $\mathbf{g}(\theta_h, \varphi_v)$ for the brevity.

kth block $\{z_{c,k,i}, z_{r,k,n}, \forall i, \forall n\}$ is given by

$$\min_{\substack{\{z_{c,k,i},\\ z_{r,k,n}\}}} \sum_{i=1}^{K} \left|\mathbf{h}_k^H \mathbf{w}_{c,i} - z_{c,k,i}\right|^2 + \sum_{n=1}^{N} \left|\mathbf{h}_k^H \mathbf{w}_{r,n} - z_{r,k,n}\right|^2 \tag{16a}$$

$$\text{s.t.} \ \frac{\left|z_{c,k,k}\right|^2}{\sum\limits_{i\neq k}^{K} \left|z_{c,k,i}\right|^2 + \sum\limits_{n=1}^{N} \left|z_{r,k,n}\right|^2 + \sigma_k^2} \geq r_{k,\text{th}}. \tag{16b}$$

It is not difficult to see that problem (16) is a quadratically constrained quadratic program (QCQP) with a convex objective function and non-convex constraint (16b). Fortunately, it was shown in [45, Appendix B.1] that strong duality holds for any optimization problem with a quadratic objective and one quadratic inequality constraint, provided that the Slater's condition holds. Therefore, we can solve problem (16) by solving its dual problem. Specifically, by introducing dual variable $\mu_1 \geq 0$ associated with constraint (16b), the Lagrangian function of problem (16) is given by

$$\begin{aligned}
&\mathcal{L}_1\left(z_{c,k,i}, z_{r,k,n}, \mu_1\right) \\
&= \sum_{i=1}^{K} \left|\mathbf{h}_k^H \mathbf{w}_{c,k} - z_{c,k,i}\right|^2 + \sum_{n=1}^{N} \left|\mathbf{h}_k^H \mathbf{w}_{r,n} - z_{r,k,n}\right|^2 + \mu_1 \\
&\quad \times \left(r_{k,\text{th}} \left(\sum_{i\neq k}^{K} \left|z_{c,k,i}\right|^2 + \sum_{n=1}^{N} \left|z_{r,k,n}\right|^2 + \sigma_k^2 \right) - \left|z_{c,k,k}\right|^2 \right).
\end{aligned} \tag{17}$$

Accordingly, the corresponding dual function is given by $\min\limits_{z_{c,k,i}, z_{r,k,n}} \mathcal{L}_1\left(z_{c,k,i}, z_{r,k,n}, \mu_1\right)$. It can be readily checked that to make the dual function bounded, we must have $0 \leq \mu_1 < 1$. Taking the first-order derivative of $\mathcal{L}_1\left(z_{c,k,i}, z_{r,k,n}, \mu_1\right)$ w.r.t. $z_{c,k,i}$ and $z_{r,k,n}$ and setting both to zero, we obtain the optimal solution as

$$z_{c,k,i}^{\text{opt}}\left(\mu_1\right) = \begin{cases} \dfrac{\mathbf{h}_k^H \mathbf{w}_{c,i}}{1 + \mu_1 r_{k,\text{th}}}, i \neq k, i \in \mathcal{K}, \\ \dfrac{\mathbf{h}_k^H \mathbf{w}_{c,k}}{1 - \mu_1}, i = k, \end{cases} \tag{18}$$

$$z_{r,k,n}^{\text{opt}}\left(\mu_1\right) = \frac{\mathbf{h}_k^H \mathbf{w}_{r,n}}{1 + \mu_1 r_{k,\text{th}}}, n \in \mathcal{N}. \tag{19}$$

If constraint (16b) is not met with equality at the optimal solution, i.e., $\mu_1^{\text{opt}} = 0$, then the optimal solutions to problem (16) are given by $z_{c,k,i}^{\text{opt}}(0)$ and $z_{r,k,n}^{\text{opt}}(0)$. Otherwise, the optimal μ_1^{opt} is a positive value ($0 < \mu_1^{\text{opt}} < 1$) that satisfies the equality constraint (16b), i.e.,

$$\begin{aligned}
&r_{k,\text{th}} \left(\sum_{i\neq k}^{K} \left|z_{c,k,i}^{\text{opt}}\left(\mu_1^{\text{opt}}\right)\right|^2 + \sum_{n=1}^{N} \left|z_{r,k,n}^{\text{opt}}\left(\mu_1^{\text{opt}}\right)\right|^2 + \sigma_k^2 \right) \\
&\qquad - \left|z_{c,k,k}^{\text{opt}}\left(\mu_1^{\text{opt}}\right)\right|^2 = 0.
\end{aligned} \tag{20}$$

It can be readily verified that $\left|z_{c,k,i}^{\text{opt}}\left(\mu_1\right)\right|^2$ for $i \neq k$ and $z_{r,k,n}^{\text{opt}}\left(\mu_1\right)$ are both monotonically decreasing with μ_1, while $z_{c,k,k}^{\text{opt}}\left(\mu_1\right)$ is monotonically increasing with μ_1 for $0 < \mu_1 < 1$. As such, the optimal μ_1^{opt} can be obtained by applying a simple bisection search method between 0 and 1.

The subproblem corresponding to block $\{y_{c,k}, y_{r,n}, \forall k, \forall n\}$ is given by

$$\begin{aligned}
\max_{\{y_{c,k}, y_{r,n}\}} &\sum_{k=1}^{K} \left|y_{c,k}\right|^2 + \sum_{n=1}^{N} \left|y_{r,n}\right|^2 - \frac{1}{2\rho} \left(\sum_{k=1}^{K} \left|\mathbf{g}^H \mathbf{w}_{c,k} - y_{c,k}\right|^2 \right. \\
&\left. + \sum\nolimits_{n=1}^{N} \left|\mathbf{g}^H \mathbf{w}_{r,n} - y_{r,n}\right|^2 \right)
\end{aligned} \tag{21a}$$

$$\text{s.t. (13c)}. \tag{21b}$$

It is observed that the objective function (21a) is a difference of two convex (DC) functions, which is non-convex. To solve it, the successive convex approximation (SCA) technique is applied. Specifically, for any given points $y_{c,k}^r$ and $y_{r,n}^r$, we have

$$\left|y_{c,k}\right|^2 \geq -\left|y_{c,k}^r\right|^2 + 2\text{Re}\left\{y_{c,k}^H y_{c,k}^r\right\} \triangleq f_1^{\text{lb}}\left(y_{c,k}\right), \quad \forall k, \tag{22}$$

$$\left|y_{r,n}\right|^2 \geq -\left|y_{r,n}^r\right|^2 + 2\text{Re}\left\{y_{r,n}^H y_{r,n}^r\right\} \triangleq f_2^{\text{lb}}\left(y_{r,n}\right), \quad \forall n. \tag{23}$$

As a result, problem (21) can be approximated as

$$\begin{aligned}
\max_{\{y_{c,k}, y_{r,n}\}} &\sum\nolimits_{k=1}^{K} f_1^{\text{lb}}\left(y_{c,k}\right) + \sum\nolimits_{n=1}^{N} f_2^{\text{lb}}\left(y_{r,n}\right) - \frac{1}{2\rho} \\
&\times \sum\nolimits_{k=1}^{K} \left|\mathbf{g}^H \mathbf{w}_{c,k} - y_{c,k}\right|^2 + \sum\nolimits_{n=1}^{N} \left|\mathbf{g}^H \mathbf{w}_{r,n} - y_{r,n}\right|^2
\end{aligned} \tag{24a}$$

$$\begin{aligned}
\text{s.t.} \ \left|y_{c,k}\right|^2 \leq r_{e,k,\text{th}} &\left(\sum_{i\neq k}^{K} f_1^{\text{lb}}\left(y_{c,i}\right) + \sum_{n=1}^{N} f_2^{\text{lb}}\left(y_{r,n}\right) + \sigma_t^2 \right), \\
&\forall k.
\end{aligned} \tag{24b}$$

It can be readily seen that problem (24) is a QCQP, which can be optimally solved by the interior-point method [45].

2) Optimizing $\{\mathbf{w}_{c,k}, \mathbf{w}_{r,n}\}$ for Given $\{v_m\}$ and Ω: This subproblem is given by (dropping irrelevant constants w.r.t. $\{\mathbf{w}_{c,k}, \mathbf{w}_{r,n}\}$)

$$\begin{aligned}
\min_{\{\mathbf{w}_{c,k}\}, \{\mathbf{w}_{r,n}\}} &\sum_{k=1}^{K} \left|\mathbf{g}^H \mathbf{w}_{c,k} - y_{c,k}\right|^2 + \sum_{n=1}^{N} \left|\mathbf{g}^H \mathbf{w}_{r,n} - y_{r,n}\right|^2 \\
&+ \sum_{k=1}^{K} \sum_{i=1}^{K} \left|\mathbf{h}_k^H \mathbf{w}_{c,i} - z_{c,k,i}\right|^2 + \sum_{k=1}^{K} \sum_{n=1}^{N} \left|\mathbf{h}_k^H \mathbf{w}_{r,n} - z_{r,k,n}\right|^2
\end{aligned} \tag{25a}$$

$$\text{s.t. (8d)}. \tag{25b}$$

Note that problem (25) is also a QCQP, which can be solved by the interior point method but with a high computational complexity [45]. To reduce the computational complexity, we obtain a semi-closed-form yet optimal solution for the transmit beamformers by using the Lagrange duality method. By introducing the dual variable $\mu_2 \geq 0$ associated with constraint (8d), the Lagrangian function of problem (25) is

given by

$$\begin{aligned}&\mathcal{L}_2\left(\mathbf{w}_{c,k},\mathbf{w}_{r,n},\mu_2\right)\\&=\sum_{k=1}^{K}\left|\mathbf{g}^H\mathbf{w}_{c,k}-y_{c,k}\right|^2+\sum_{n=1}^{N}\left|\mathbf{g}^H\mathbf{w}_{r,n}-y_{r,n}\right|^2\\&\quad+\sum_{k=1}^{K}\sum_{i=1}^{K}\left|\mathbf{h}_k^H\mathbf{w}_{c,i}-z_{c,k,i}\right|^2+\sum_{k=1}^{K}\sum_{n=1}^{N}\left|\mathbf{h}_k^H\mathbf{w}_{r,n}-z_{r,k,n}\right|^2\\&\quad+\mu_2\left(\sum_{k=1}^{K}\left\|\mathbf{w}_{c,k}\right\|^2+\sum_{n=1}^{N}\left\|\mathbf{w}_{r,n}\right\|^2-P_{\max}\right).\end{aligned}\tag{26}$$

By taking the first-order derivative of $\mathcal{L}_2\left(\mathbf{w}_{c,k},\mathbf{w}_{r,n},\mu_2\right)$ w.r.t. $\mathbf{w}_{c,k}$ and $\mathbf{w}_{r,n}$ and setting both to zero, we obtain the optimal solutions as

$$\begin{aligned}\mathbf{w}_{c,k}^{\mathrm{opt}}\left(\mu_2\right)=&\left(\mathbf{g}\mathbf{g}^H+\sum\nolimits_{i=1}^{K}\mathbf{h}_i\mathbf{h}_i^H+\mu_2\mathbf{I}_N\right)^{-1}\\&\times\left(y_{c,k}\mathbf{g}+\sum\nolimits_{i=1}^{K}z_{c,i,k}\mathbf{h}_i\right),k\in\mathcal{K},\end{aligned}\tag{27}$$

$$\begin{aligned}\mathbf{w}_{r,n}^{\mathrm{opt}}\left(\mu_2\right)=&\left(\mathbf{g}\mathbf{g}^H+\sum\nolimits_{i=1}^{K}\mathbf{h}_i\mathbf{h}_i^H+\mu_2\mathbf{I}_N\right)^{-1}\\&\times\left(y_{r,n}\mathbf{g}+\sum\nolimits_{i=1}^{K}z_{r,i,n}\mathbf{h}_i\right),n\in\mathcal{N}.\end{aligned}\tag{28}$$

Note that the optimal solution must be satisfied with the following complementary slackness condition [45]

$$\mu_2^{\mathrm{opt}}\left(P\left(\mu_2^{\mathrm{opt}}\right)-P_{\max}\right)=0,\tag{29}$$

where $P\left(\mu_1^{\mathrm{opt}}\right)=\sum\limits_{k=1}^{K}\left\|\mathbf{w}_{c,k}^{\mathrm{opt}}\left(\mu_2^{\mathrm{opt}}\right)\right\|^2+\sum\limits_{n=1}^{N}\left\|\mathbf{w}_{r,n}^{\mathrm{opt}}\left(\mu_2^{\mathrm{opt}}\right)\right\|^2$. We first check whether $\mu_2^{\mathrm{opt}}=0$ is the optimal solution or not. If $P\left(0\right)-P_{\max}<0$, it means that the optimal dual variable μ_2^{opt} equals 0; otherwise, the optimal μ_2^{opt} is a positive value that satisfies $P\left(\mu_2^{\mathrm{opt}}\right)-P_{\max}=0$, and can be obtained as follows. Let $\mathbf{S}=\mathbf{g}\mathbf{g}^H+\sum\limits_{i=1}^{K}\mathbf{h}_i\mathbf{h}_i^H$, $\mathbf{t}_{c,k}=y_{c,k}\mathbf{g}+\sum\limits_{i=1}^{K}z_{c,i,k}\mathbf{h}_i$, and $\mathbf{t}_{r,n}=y_{r,n}\mathbf{g}+\sum\limits_{i=1}^{K}z_{r,i,n}\mathbf{h}_i$, which implies

$$\begin{aligned}\left\|\mathbf{w}_{c,k}^{\mathrm{opt}}\left(\mu_2\right)\right\|^2&=\mathrm{tr}\left(\left(\mathbf{S}+\mu_2\mathbf{I}_N\right)^{-2}\mathbf{t}_{c,k}\mathbf{t}_{c,k}^H\right),\\\left\|\mathbf{w}_{r,n}^{\mathrm{opt}}\left(\mu_2\right)\right\|^2&=\mathrm{tr}\left(\left(\mathbf{S}+\mu_2\mathbf{I}_N\right)^{-2}\mathbf{t}_{r,n}\mathbf{t}_{r,n}^H\right).\end{aligned}\tag{30}$$

Since $\mathbf{S}$ is a positive semi-definite matrix, its eigendecomposition can be expressed as $\mathbf{S}=\mathbf{U}\mathbf{\Sigma}\mathbf{U}^H$. Substituting it into (30) yields

$$P\left(\mu_2\right)=\sum_{i=1}^{N}\frac{\left(\mathbf{U}^H\left(\sum\limits_{k=1}^{K}\mathbf{t}_{c,k}\mathbf{t}_{c,k}^H+\sum\limits_{n=1}^{N}\mathbf{t}_{r,n}\mathbf{t}_{r,n}^H\right)\mathbf{U}\right)_{i,i}}{\left(\mathbf{\Sigma}_{i,i}+\mu_2\right)^2}.\tag{31}$$

It can be readily seen that $P\left(\mu_2\right)$ is monotonically decreasing w.r.t. μ_2, which motivates us to apply the bisection method to search for μ_2 satisfying $P\left(\mu_2^{\mathrm{opt}}\right)=P_{\max}$. To reduce the search space, an upper bound of μ_2 can be derived as $\mu_2^{\mathrm{up}}=\sqrt{\sum\limits_{i=1}^{N}\left(\mathbf{U}^H\left(\sum\limits_{k=1}^{K}\mathbf{t}_{c,k}\mathbf{t}_{c,k}^H+\sum\limits_{n=1}^{N}\mathbf{t}_{r,n}\mathbf{t}_{r,n}^H\right)\mathbf{U}\right)_{i,i}/P_{\max}}$ by setting $\mathbf{\Sigma}_{i,i}$ in (31) to zero.

3) Optimizing $\{v_m\}$ for Given $\{\mathbf{w}_{c,k},\mathbf{w}_{r,n}\}$ and Ω: This subproblem is given by (ignoring the constant terms w.r.t. $\{v_m\}$)

$$\begin{aligned}\min_{\{v_m\}}&\sum_{k=1}^{K}\left|\mathbf{g}^H\mathbf{w}_{c,k}-y_{c,k}\right|^2+\sum_{n=1}^{N}\left|\mathbf{g}^H\mathbf{w}_{r,n}-y_{r,n}\right|^2\\&+\sum_{k=1}^{K}\sum_{i=1}^{K}\left|\mathbf{h}_k^H\mathbf{w}_{c,i}-z_{c,k,i}\right|^2+\sum_{k=1}^{K}\sum_{n=1}^{N}\left|\mathbf{h}_k^H\mathbf{w}_{r,n}-z_{r,k,n}\right|^2\end{aligned}\tag{32a}$$

$$\text{s.t. (8e).}\tag{32b}$$

Although the objective function (32a) is a quadratic function of $\mathbf{v}$, the unit-modulus constraint imposed on each IRS phase shift in (8e) is non-convex. Here, we construct an upper-bounded convex surrogate function for (32a) by applying the MM algorithm [46], based on which a closed-form solution for the IRS phase shifts is derived. Specifically, the surrogate function at any given point $\mathbf{v}^r$, denoted by $\varpi\left(\mathbf{v}|\mathbf{v}^r\right)$, for a quadratic function $\mathbf{v}^H\mathbf{A}\mathbf{v}$ can be expressed as

$$\begin{aligned}\varpi\left(\mathbf{v}|\mathbf{v}^r\right)=&\lambda_{\max}\mathbf{v}^H\mathbf{v}-2\mathrm{Re}\left\{\mathbf{v}^H\left(\lambda_{\max}\mathbf{I}_M-\mathbf{A}\right)\mathbf{v}^r\right\}\\&+\mathbf{v}^{r,H}\left(\lambda_{\max}\mathbf{I}_M-\mathbf{A}\right)\mathbf{v}^r,\end{aligned}\tag{33}$$

where $\mathbf{A}\in\mathbb{C}^{M\times M}$ is positive semi-definite, and $\lambda_{\max}$ is the maximum eigenvalue of $\mathbf{A}$. As a result, based on $\mathbf{v}^H\mathbf{v}=M$, we can solve the following approximate optimization problem (ignoring constant terms w.r.t. $\{v_m\}$)

$$\max_{v_m}\ \mathrm{Re}\left\{\mathbf{v}^H\mathbf{q}^r\right\}\tag{34a}$$

$$\text{s.t. (8e),}\tag{34b}$$

where $\mathbf{q}^r=\sum_{k=1}^{K}\left(\left(\lambda_{\max,1,k}\mathbf{I}_M-\Upsilon_{r,c,k}\right)\mathbf{v}^r+y_{c,k}^H\mathbf{F}_r\mathbf{w}_{c,k}\right)+\sum_{n=1}^{N}\left(\left(\lambda_{\max,2,n}\mathbf{I}_M-\Upsilon_{r,r,n}\right)\mathbf{v}^r+y_{r,n}^H\mathbf{F}_r\mathbf{w}_{r,n}\right)+\sum_{k=1}^{K}\sum_{i=1}^{K}\left(\left(\lambda_{\max,3,k}\mathbf{I}_M-\Upsilon_{c,k,i}\right)\mathbf{v}^r-\Psi_{c,k,i}\right)+\sum_{k=1}^{K}\sum_{n=1}^{N}\left(\left(\lambda_{\max,4,k,n}\mathbf{I}_M-\Upsilon_{r,k,n}\right)\mathbf{v}^r-\Psi_{r,n,k}\right)$, $\Psi_{c,k,i}=\mathbf{F}_k\mathbf{w}_{c,i}\left(\mathbf{w}_{c,i}^H\mathbf{h}_{d,k}-z_{c,k,i}^H\right)$, $\Psi_{r,n,k}=\mathbf{F}_k\mathbf{w}_{r,n}\left(\mathbf{w}_{r,n}^H\mathbf{h}_{d,k}-z_{r,k,n}^H\right)$, $\Upsilon_{r,c,k}=\mathbf{F}_r\mathbf{w}_{c,k}\mathbf{w}_{c,k}^H\mathbf{F}_r^H$, $\Upsilon_{r,r,n}=\mathbf{F}_r\mathbf{w}_{r,n}\mathbf{w}_{r,n}^H\mathbf{F}_r^H$, $\Upsilon_{c,k,i}=\mathbf{F}_k\mathbf{w}_{c,i}\mathbf{w}_{c,i}^H\mathbf{F}_k^H$, $\Upsilon_{r,k,n}=\mathbf{F}_k\mathbf{w}_{r,n}\mathbf{w}_{r,n}^H\mathbf{F}_k^H$, and $\lambda_{\max,1,k}$, $\lambda_{\max,2,n}$, $\lambda_{\max,3,k,i}$, and $\lambda_{\max,4,k,n}$ represent the maximum eigenvalues of $\Upsilon_{r,c,k}$, $\Upsilon_{r,r,n}$, $\Upsilon_{c,k,i}$, and $\Upsilon_{r,k,n}$, respectively. The optimal solution $\mathbf{v}$ to problem (34) is then given by

$$\mathbf{v}^{\mathrm{opt}}=e^{j\arg\left(\mathbf{q}^r\right)}.\tag{35}$$

B. Outer Layer Optimization

In the outer layer, the penalty parameter in the rth iteration is updated as follows

$$\rho^r=c\rho^{r-1},\ 0<c<1,\tag{36}$$

where c is a constant scaling factor that is used to control the convergence behavior.

Algorithm 1 Penalty-Based Algorithm for Solving Problem (8)

1: **Initialize** $\mathbf{v}$, $\{\mathbf{w}_{c,k}, \mathbf{w}_{r,n}\}$, $\{y_{c,k}, y_{r,n}\}$, c, ρ, ε_{in}, and ε_{out}.
2: **repeat: outer layer**
3: **repeat: inner layer**
4: Update auxiliary variables $\{z_{c,k,i}, z_{r,k,n}\}$ by solving problem (16).
5: Update auxiliary variables $\{y_{c,k}, y_{r,n}\}$ by solving problem (24).
6: Update transmit beamformers $\{\mathbf{w}_{c,k}, \mathbf{w}_{r,n}\}$ by solving problem (25).
7: Update IRS phase shifts $\{v_m\}$ based on (35).
8: **until** the fractional increase of the objective value of (14) is below a threshold ε_{in}.
9: Update penalty parameter ρ based on (36).
10: **until** termination indicator ξ defined in (37) is below a threshold ε_{out}.

C. Overall Algorithm and Computational Complexity

The termination indicator for the penalty-based algorithm is given by

$$\xi = \max_{\forall i,k,n} \Big\{ \left|\mathbf{g}^H \mathbf{w}_{c,k} - y_{c,k}\right|^2, \left|\mathbf{g}^H \mathbf{w}_{r,n} - y_{r,n}\right|^2, \left|\mathbf{h}_k^H \mathbf{w}_{c,i} - z_{c,k,i}\right|^2, \left|\mathbf{h}_k^H \mathbf{w}_{r,n} - z_{r,k,n}\right|^2 \Big\}. \quad (37)$$

If ξ is smaller than a predefined value, constraint (13d) is considered to be met with equality for a given accuracy. The proposed algorithm is summarized in Algorithm 1.

In Algorithm 1, each block in the inner layer is locally and/or optimally solved and the objective value of problem (14) is thus non-decreasing over iterations in each inner layer. In addition, the optimal objective value of problem (8) is upper-bounded by a finite value due to the limited transmit power. Following [47, Theorem 4.1], the solution obtained by Algorithm 1 is guaranteed to converge to a stationary point. In additin, the computational complexity is given by $\mathcal{O}\left(I_{\text{out}} I_{\text{in}} \left(K \log_2\left(\frac{1}{\varepsilon}\right) N^3 + \log_2\left(\frac{\mu_2^{\text{up}}}{\varepsilon}\right) N^3 + (K+N)^{3.5} + M^3\right)\right)$, where ε represents the iteration accuracy, and I_{in} and I_{out} denote the numbers of iterations required for reaching convergence in the inner layer and outer layer, respectively.

IV. Proposed Solution for Imperfect CSI and Uncertain Target Location

In this section, we consider the case with imperfect CSI and uncertain target location. Since problem (12) involves an infinite number of inequalities in constraints (12b) and (12c), the previous penalty-based algorithm is no longer applicable for solving problem (12), which thus calls for new algorithm design. By introducing auxiliary variables $\{\beta_{c,k} \geq 0\}$ satisfying $\beta_{c,k} = \sum_{i \neq k}^{K} \left|\mathbf{h}_k^H \mathbf{w}_{c,i}\right|^2 + \sum_{n=1}^{N} \left|\mathbf{h}_k^H \mathbf{w}_{r,n}\right|^2 + \sigma_k^2, k \in \mathcal{K}$, constraint (12b) can be equivalently transformed as

$$\left|\mathbf{h}_k^H \mathbf{w}_{c,k}\right|^2 \geq \beta_{c,k} r_{k,\text{th}}, \quad \Delta\mathbf{h}_{d,k} \in \mathcal{H}_{d,k},\ \Delta\mathbf{F}_k \in \mathcal{F}_k,\ k \in \mathcal{K}, \quad (38)$$

$$\sum_{i \neq k}^{K} \left|\mathbf{h}_k^H \mathbf{w}_{c,i}\right|^2 + \sum_{n=1}^{N} \left|\mathbf{h}_k^H \mathbf{w}_{r,n}\right|^2 + \sigma_k^2 \leq \beta_{c,k}, \quad \Delta\mathbf{h}_{d,k} \in \mathcal{H}_{d,k},\ \Delta\mathbf{F}_k \in \mathcal{F}_k,\ k \in \mathcal{K}. \quad (39)$$

Although the left-hand side of (38) is convex w.r.t $\mathbf{v}$ (recall that $\mathbf{h}_k^H = \mathbf{v}^H \mathbf{F}_k + \mathbf{h}_{d,k}^H$), the resulting set is not a convex set since the superlevel set of a convex quadratic function is not convex in general. To address this non-convex constraint, we take the first-order Taylor expansion of $\left|\mathbf{h}_k^H \mathbf{w}_{c,k}\right|^2$ at any given feasible point $\mathbf{v}^r$ to obtain the following lower bound

$$\begin{aligned}&\left|\mathbf{h}_k^H \mathbf{w}_{c,k}\right|^2 \\ &\geq f_k^{\text{lb}}(\mathbf{v}) \triangleq -\left|\mathbf{v}^{r,H} \mathbf{F}_k \mathbf{w}_{c,k}^r + \mathbf{h}_{d,k}^H \mathbf{w}_{c,k}^r\right|^2 + 2\text{Re}\Big\{ \\ &\quad \left(\mathbf{v}^H \mathbf{F}_k \mathbf{w}_{c,k} + \mathbf{h}_{d,k}^H \mathbf{w}_{c,k}\right)^H \left(\mathbf{v}^{r,H} \mathbf{F}_k \mathbf{w}_{c,k}^r + \mathbf{h}_{d,k}^H \mathbf{w}_{c,k}^r\right) \Big\},\end{aligned} \quad (40)$$

which is linear and convex w.r.t. $\mathbf{v}$.

Substituting $\mathbf{F}_k = \hat{\mathbf{F}}_k + \Delta\mathbf{F}_k$ and $\mathbf{h}_{d,k} = \hat{\mathbf{h}}_{d,k} + \Delta\mathbf{h}_{d,k}$ into term $\left|\mathbf{v}^{r,H} \mathbf{F}_k \mathbf{w}_{c,k}^r + \mathbf{h}_{d,k}^H \mathbf{w}_{c,k}^r\right|^2$ in (40), we can rewrite it as

$$\begin{aligned}&\left|\mathbf{v}^{r,H} \mathbf{F}_k \mathbf{w}_{c,k}^r + \mathbf{h}_{d,k}^H \mathbf{w}_{c,k}^r\right|^2 \\ &= \left|\hat{\mathbf{h}}_k^{r,H} \mathbf{w}_{c,k}^r\right|^2 + \left|\mathbf{v}^{r,H} \Delta\mathbf{F}_k \mathbf{w}_{c,k}^r + \Delta\mathbf{h}_{d,k}^H \mathbf{w}_{c,k}^r\right|^2 \\ &\quad + 2\text{Re}\left\{ \left(\hat{\mathbf{h}}_k^{r,H} \mathbf{w}_{c,k}^r\right)^H \left(\mathbf{v}^{r,H} \Delta\mathbf{F}_k \mathbf{w}_{c,k}^r + \Delta\mathbf{h}_{d,k}^H \mathbf{w}_{c,k}^r\right) \right\},\end{aligned} \quad (41)$$

where $\hat{\mathbf{h}}_k^{r,H} = \mathbf{v}^{r,H} \hat{\mathbf{F}}_k + \hat{\mathbf{h}}_{d,k}^H$. Below, we rewrite terms in (41) into a compact form that facilitates the algorithm design. Specifically, we first expand $\left|\mathbf{v}^{r,H} \Delta\mathbf{F}_k \mathbf{w}_{c,k}^r + \Delta\mathbf{h}_{d,k}^H \mathbf{w}_{c,k}^r\right|^2$ as

$$\begin{aligned}&\left|\mathbf{v}^{r,H} \Delta\mathbf{F}_k \mathbf{w}_{c,k}^r + \Delta\mathbf{h}_{d,k}^H \mathbf{w}_{c,k}^r\right|^2 \\ &= \mathbf{v}^{r,H} \Delta\mathbf{F}_k \mathbf{w}_{c,k}^r \mathbf{w}_{c,k}^{r,H} \Delta\mathbf{F}_k^H \mathbf{v}^r \\ &\quad + \Delta\mathbf{h}_{d,k}^H \mathbf{w}_{c,k}^r \mathbf{w}_{c,k}^{r,H} \Delta\mathbf{h}_{d,k} + \mathbf{v}^{r,H} \Delta\mathbf{F}_k \mathbf{w}_{c,k}^r \mathbf{w}_{c,k}^{r,H} \Delta\mathbf{h}_{d,k} \\ &\quad + \Delta\mathbf{h}_{d,k}^H \mathbf{w}_{c,k}^r \mathbf{w}_{c,k}^{r,H} \Delta\mathbf{F}_k^H \mathbf{v}^r,\end{aligned} \quad (42)$$

where

$$\begin{aligned}&\mathbf{v}^{r,H} \Delta\mathbf{F}_k \mathbf{w}_{c,k}^r \mathbf{w}_{c,k}^{r,H} \Delta\mathbf{F}_k^H \mathbf{v}^r \\ &= \text{vec}^H(\Delta\mathbf{F}_k^*) \left(\mathbf{w}_{c,k}^r \mathbf{w}_{c,k}^{r,H}\right) \otimes \left(\mathbf{v}^{r,*} \mathbf{v}^{r,T}\right) \text{vec}(\Delta\mathbf{F}_k^*),\end{aligned} \quad (43)$$

$$\begin{aligned}&\mathbf{v}^{r,H} \Delta\mathbf{F}_k \mathbf{w}_{c,k}^r \mathbf{w}_{c,k}^{r,H} \Delta\mathbf{h}_{d,k} \\ &= \text{vec}^H(\Delta\mathbf{F}_k^*) \left(\left(\mathbf{w}_{c,k}^r \mathbf{w}_{c,k}^{r,H}\right) \otimes \mathbf{v}^{r,*}\right) \Delta\mathbf{h}_{d,k},\end{aligned} \quad (44)$$

$$\begin{aligned}&\Delta\mathbf{h}_{d,k}^H \mathbf{w}_{c,k}^r \mathbf{w}_{c,k}^{r,H} \Delta\mathbf{F}_k^H \mathbf{v}^r \\ &= \Delta\mathbf{h}_{d,k}^H \left(\left(\mathbf{w}_{c,k}^r \mathbf{w}_{c,k}^{r,H}\right) \otimes \mathbf{v}^{r,T}\right) \text{vec}(\Delta\mathbf{F}_k^*).\end{aligned} \quad (45)$$

Thus, we can rewrite $\left|\mathbf{v}^{r,H}\Delta\mathbf{F}_k\mathbf{w}_{c,k}^r+\Delta\mathbf{h}_{d,k}^H\mathbf{w}_{c,k}^r\right|^2$ in a more compact form given by

$$\left|\mathbf{v}^{r,H}\Delta\mathbf{F}_k\mathbf{w}_{c,k}^r+\Delta\mathbf{h}_{d,k}^H\mathbf{w}_{c,k}^r\right|^2=\Delta\mathbf{h}_{k,\text{eff}}^H\mathbf{H}_{c,k}^r\Delta\mathbf{h}_{k,\text{eff}}, \tag{46}$$

where $\Delta\mathbf{h}_{k,\text{eff}}^H=\left[\Delta\mathbf{h}_{d,k}^H\text{vec}^H\left(\Delta\mathbf{F}_k^*\right)\right]$, $\mathbf{H}_{c,k}^r=\begin{bmatrix}\mathbf{w}_{c,k}^r\mathbf{w}_{c,k}^{r,H} & \left(\mathbf{w}_{c,k}^r\mathbf{w}_{c,k}^{r,H}\right)\otimes\mathbf{v}^{r,T}\\ \left(\mathbf{w}_{c,k}^r\mathbf{w}_{c,k}^{r,H}\right)\otimes\mathbf{v}^{r,*} & \left(\mathbf{w}_{c,k}^r\mathbf{w}_{c,k}^{r,H}\right)\otimes\left(\mathbf{v}^{r,*}\mathbf{v}^{r,T}\right)\end{bmatrix}$. Then, $\left(\hat{\mathbf{h}}_k^{r,H}\mathbf{w}_{c,k}^r\right)^H\left(\mathbf{v}^{r,H}\Delta\mathbf{F}_k\mathbf{w}_{c,k}^r+\Delta\mathbf{h}_{d,k}^H\mathbf{w}_{c,k}^r\right)$ can be expressed as

$$\begin{aligned}&\left(\hat{\mathbf{h}}_k^{r,H}\mathbf{w}_{c,k}^r\right)^H\left(\mathbf{v}^{r,H}\Delta\mathbf{F}_k\mathbf{w}_{c,k}^r+\Delta\mathbf{h}_{d,k}^H\mathbf{w}_{c,k}^r\right)\\&\quad=\left(\hat{\mathbf{h}}_k^{r,H}\mathbf{w}_{c,k}^r\right)^H\Delta\mathbf{h}_{k,\text{eff}}^H\mathbf{h}_{c,k}^r,\end{aligned} \tag{47}$$

where $\mathbf{h}_{c,k}^r=\left[\mathbf{w}_{c,k}^{r,T}\left(\mathbf{w}_{c,k}^r\otimes\mathbf{v}^{r,H}\right)\right]^T$.

Based on (41), (46), and (47), we can compactly rewrite $\left|\mathbf{v}^{r,H}\mathbf{F}_k\mathbf{w}_{c,k}^r+\mathbf{h}_{d,k}^H\mathbf{w}_{c,k}^r\right|^2$ in (41) as

$$\begin{aligned}&\left|\mathbf{v}^{r,H}\mathbf{F}_k\mathbf{w}_{c,k}^r+\mathbf{h}_{d,k}^H\mathbf{w}_{c,k}^r\right|^2\\&\quad=\Delta\mathbf{h}_{k,\text{eff}}^H\mathbf{H}_{c,k}^r\Delta\mathbf{h}_{k,\text{eff}}\\&\qquad+2\text{Re}\left\{\left(\hat{\mathbf{h}}_k^{r,H}\mathbf{w}_{c,k}^r\right)^H\Delta\mathbf{h}_{k,\text{eff}}^H\mathbf{h}_{c,k}^r\right\}+\left|\hat{\mathbf{h}}_k^{r,H}\mathbf{w}_{c,k}^r\right|^2.\end{aligned} \tag{48}$$

In addition, we can expand $\left(\mathbf{v}^H\mathbf{F}_k\mathbf{w}_{c,k}+\mathbf{h}_{d,k}^H\mathbf{w}_{c,k}\right)^H\times\left(\mathbf{v}^{r,H}\mathbf{F}_k\mathbf{w}_{c,k}^r+\mathbf{h}_{d,k}^H\mathbf{w}_{c,k}^r\right)$ in (40) as

$$\begin{aligned}&\left(\mathbf{v}^H\mathbf{F}_k\mathbf{w}_{c,k}+\mathbf{h}_{d,k}^H\mathbf{w}_{c,k}\right)^H\left(\mathbf{v}^{r,H}\mathbf{F}_k\mathbf{w}_{c,k}^r+\mathbf{h}_{d,k}^H\mathbf{w}_{c,k}^r\right)\\&\quad=\mathbf{w}_{c,k}^H\hat{\mathbf{h}}_k\hat{\mathbf{h}}_k^{r,H}\mathbf{w}_{c,k}^r+\mathbf{w}_{c,k}^H\hat{\mathbf{h}}_k\mathbf{v}^{r,H}\Delta\mathbf{F}_k\mathbf{w}_{c,k}^r\\&\qquad+\mathbf{w}_{c,k}^H\hat{\mathbf{h}}_k\Delta\mathbf{h}_{d,k}^H\mathbf{w}_{c,k}^r+\mathbf{w}_{c,k}^H\Delta\mathbf{F}_k^H\mathbf{v}\hat{\mathbf{h}}_k^{r,H}\mathbf{w}_{c,k}^r\\&\qquad+\mathbf{w}_{c,k}^H\Delta\mathbf{F}_k^H\mathbf{v}\mathbf{v}^{r,H}\Delta\mathbf{F}_k\mathbf{w}_{c,k}^r+\mathbf{w}_{c,k}^H\Delta\mathbf{F}_k^H\mathbf{v}\Delta\mathbf{h}_{d,k}^H\mathbf{w}_{c,k}^r\\&\qquad+\mathbf{w}_{c,k}^H\Delta\mathbf{h}_{d,k}\hat{\mathbf{h}}_k^{r,H}\mathbf{w}_{c,k}^r+\mathbf{w}_{c,k}^H\Delta\mathbf{h}_{d,k}\mathbf{v}^{r,H}\Delta\mathbf{F}_k\mathbf{w}_{c,k}^r\\&\qquad+\mathbf{w}_{c,k}^H\Delta\mathbf{h}_{d,k}\Delta\mathbf{h}_{d,k}^H\mathbf{w}_{c,k}^r,\end{aligned} \tag{49}$$

where $\hat{\mathbf{h}}_k^H=\mathbf{v}^H\hat{\mathbf{F}}_k+\hat{\mathbf{h}}_{d,k}^H$. Similarly, we can transform terms in (49) as

$$\begin{aligned}&\mathbf{w}_{c,k}^H\hat{\mathbf{h}}_k\mathbf{v}^{r,H}\Delta\mathbf{F}_k\mathbf{w}_{c,k}^r\\&\quad=\text{vec}^H\left(\Delta\mathbf{F}_k^*\right)\left(\mathbf{w}_{c,k}^{r,T}\otimes\mathbf{v}^{r,H}\right)^T\mathbf{w}_{c,k}^H\hat{\mathbf{h}}_k,\end{aligned} \tag{50}$$

$$\begin{aligned}&\mathbf{w}_{c,k}^H\Delta\mathbf{F}_k^H\mathbf{v}\hat{\mathbf{h}}_k^{r,H}\mathbf{w}_{c,k}^r\\&\quad=\hat{\mathbf{h}}_k^{r,H}\mathbf{w}_{c,k}^r\left(\mathbf{w}_{c,k}^H\otimes\mathbf{v}^T\right)\text{vec}\left(\Delta\mathbf{F}_k^*\right),\end{aligned} \tag{51}$$

$$\begin{aligned}&\mathbf{w}_{c,k}^H\Delta\mathbf{F}_k^H\mathbf{v}\mathbf{v}^{r,H}\Delta\mathbf{F}_k\mathbf{w}_{c,k}^r\\&\quad=\text{vec}^H\left(\Delta\mathbf{F}_k^*\right)\left(\left(\mathbf{w}_{c,k}^r\mathbf{w}_{c,k}^H\right)^T\otimes\left(\mathbf{v}\mathbf{v}^{r,H}\right)\right)^T\text{vec}\left(\Delta\mathbf{F}_k^*\right),\end{aligned} \tag{52}$$

$$\begin{aligned}&\mathbf{w}_{c,k}^H\Delta\mathbf{F}_k^H\mathbf{v}\Delta\mathbf{h}_{d,k}^H\mathbf{w}_{c,k}^r\\&\quad=\Delta\mathbf{h}_{d,k}^H\left(\left(\mathbf{w}_{c,k}^r\mathbf{w}_{c,k}^H\right)^T\otimes\mathbf{v}\right)^T\text{vec}\left(\Delta\mathbf{F}_k^*\right).\end{aligned} \tag{53}$$

Thus, $\left(\mathbf{v}^H\mathbf{F}_k\mathbf{w}_{c,k}+\mathbf{h}_{d,k}^H\mathbf{w}_{c,k}\right)^H\left(\mathbf{v}^{r,H}\mathbf{F}_k\mathbf{w}_{c,k}^r+\mathbf{h}_{d,k}^H\mathbf{w}_{c,k}^r\right)$ can be written in a more compact form given by

$$\begin{aligned}&\left(\mathbf{v}^H\mathbf{F}_k\mathbf{w}_{c,k}+\mathbf{h}_{d,k}^H\mathbf{w}_{c,k}\right)^H\left(\mathbf{v}^{r,H}\mathbf{F}_k\mathbf{w}_{c,k}^r+\mathbf{h}_{d,k}^H\mathbf{w}_{c,k}^r\right)\\&\quad=\Delta\mathbf{h}_{k,\text{eff}}^H\mathbf{H}_{c,k}\Delta\mathbf{h}_{k,\text{eff}}+\Delta\mathbf{h}_{k,\text{eff}}^H\mathbf{h}_{c,k}^r\mathbf{w}_{c,k}^H\hat{\mathbf{h}}_k\\&\qquad+\hat{\mathbf{h}}_k^{r,H}\mathbf{w}_{c,k}^r\mathbf{h}_{c,k}^H\Delta\mathbf{h}_{k,\text{eff}}+\mathbf{w}_{c,k}^H\hat{\mathbf{h}}_k\hat{\mathbf{h}}_k^{r,H}\mathbf{w}_{c,k}^r,\end{aligned} \tag{54}$$

where $\mathbf{h}_{c,k}=\left[\mathbf{w}_{c,k}^T\left(\mathbf{w}_{c,k}^T\otimes\mathbf{v}^H\right)\right]^T$ and $\mathbf{H}_{c,k}=\begin{bmatrix}\mathbf{w}_{c,k}^r\mathbf{w}_{c,k}^H & \left(\mathbf{w}_{c,k}^r\mathbf{w}_{c,k}^H\right)\otimes\mathbf{v}^T\\ \left(\mathbf{w}_{c,k}^r\mathbf{w}_{c,k}^H\right)\otimes\mathbf{v}^{r,*} & \left(\mathbf{w}_{c,k}^r\mathbf{w}_{c,k}^H\right)\otimes\left(\mathbf{v}^{r,*}\mathbf{v}^T\right)\end{bmatrix}$.

As a result, based on (40), (48), and (54), constraint (38) can be approximated as

$$\begin{aligned}&\Delta\mathbf{h}_{k,\text{eff}}^H\left(\mathbf{H}_{c,k}+\mathbf{H}_{c,k}^H-\mathbf{H}_{c,k}^r\right)\Delta\mathbf{h}_{k,\text{eff}}+2\text{Re}\left\{\hat{\mathbf{h}}_{c,k}^H\Delta\mathbf{h}_{k,\text{eff}}\right\}\\&\quad+\bar{h}_{c,k}\geq\beta_{c,k}r_{k,\text{th}},\Delta\mathbf{h}_{d,k}\in\mathcal{H}_{d,k},\Delta\mathbf{F}_k\in\mathcal{F}_k,k\in\mathcal{K},\end{aligned} \tag{55}$$

where $\hat{\mathbf{h}}_{c,k}^H=\hat{\mathbf{h}}_k^H\mathbf{w}_{c,k}\mathbf{h}_{c,k}^{r,H}+\hat{\mathbf{h}}_k^{r,H}\mathbf{w}_{c,k}^r\mathbf{h}_{c,k}^H-\hat{\mathbf{h}}_k^{r,H}\mathbf{w}_{c,k}^r\mathbf{h}_{c,k}^{r,H}$ and $\bar{h}_{c,k}=2\text{Re}\left\{\mathbf{w}_{c,k}^H\hat{\mathbf{h}}_k\hat{\mathbf{h}}_k^{r,H}\mathbf{w}_{c,k}^r\right\}-\left|\hat{\mathbf{h}}_k^{r,H}\mathbf{w}_{c,k}^r\right|^2$. We note that (55) still involves an infinite number of inequality constraints. To circumvent this difficulty, we convert the infinite number of constraints in (55) into an equivalent form with only a finite number of LMIs by applying the following lemma.

Lemma 1 (General S-Procedure [48]): Let $f_i(\mathbf{z})=\mathbf{z}^H\mathbf{A}_i\mathbf{z}+2\text{Re}\left\{\mathbf{b}_i^H\mathbf{z}\right\}+c_i,i\in\{0,1,\ldots,\text{I}\}$, where $\mathbf{z}\in\mathbb{C}^{N\times1}$ and $\mathbf{A}_i=\mathbf{A}_i^H\in\mathbb{C}^{N\times N}$. The condition $\{f_1(\mathbf{z})\geq0\}_{i=1}^{\text{I}}\Rightarrow f_0(\mathbf{z})\geq0$ holds if and only if there exist $\lambda_i\geq0,i\in\{1,\ldots,\text{I}\}$ such that

$$\begin{bmatrix}\mathbf{A}_0 & \mathbf{b}_0\\ \mathbf{b}_0^H & c_0\end{bmatrix}-\sum_{i=1}^{\text{I}}\lambda_i\begin{bmatrix}\mathbf{A}_i & \mathbf{b}_i\\ \mathbf{b}_i^H & c_i\end{bmatrix}\succeq\mathbf{0}_{N+1}. \tag{56}$$

Before applying Lemma 1, we first re-express uncertainties $\Delta\mathbf{h}_{d,k}\in\mathcal{H}_{d,k}$ and $\Delta\mathbf{F}_k\in\mathcal{F}_k$ as

$$\begin{aligned}&\Delta\mathbf{h}_{d,k}\in\mathcal{H}_{d,k}\\&\Rightarrow\Delta\mathbf{h}_{k,\text{eff}}^H\begin{bmatrix}\mathbf{I}_N & \mathbf{0}_{N\times MN}\\ \mathbf{0}_{MN\times N} & \mathbf{0}_{MN}\end{bmatrix}\Delta\mathbf{h}_{k,\text{eff}}\leq\varepsilon_{d,k}^2,k\in\mathcal{K},\end{aligned} \tag{57}$$

$$\begin{aligned}&\Delta\mathbf{F}_k\in\mathcal{F}_k\\&\Rightarrow\Delta\mathbf{h}_{k,\text{eff}}^H\begin{bmatrix}\mathbf{0}_N & \mathbf{0}_{N\times MN}\\ \mathbf{0}_{MN\times N} & \mathbf{I}_{MN}\end{bmatrix}\Delta\mathbf{h}_{k,\text{eff}}\leq\varepsilon_k^2,k\in\mathcal{K}.\end{aligned} \tag{58}$$

Then, based on Lemma 1, (55) can be transformed as

$$\begin{bmatrix}\mathbf{H}_{c,k}+\mathbf{H}_{c,k}^H-\mathbf{H}_{c,k}^r+\begin{bmatrix}\lambda_{1,k}\mathbf{I}_N & \mathbf{0}_{N\times MN}\\ \mathbf{0}_{MN\times N} & \lambda_{2,k}\mathbf{I}_{MN}\end{bmatrix} & \hat{\mathbf{h}}_{c,k}\\ \hat{\mathbf{h}}_{c,k}^H & c_k\end{bmatrix}\succeq\mathbf{0}_{N+MN+1},k\in\mathcal{K}, \tag{59}$$

where $c_k=\bar{h}_{c,k}-\beta_{c,k}r_{k,\text{th}}-\lambda_{1,k}\varepsilon_{d,k}^2-\lambda_{2,k}\varepsilon_k^2$, $\lambda_{1,k}\geq0$ and $\lambda_{1,k}\geq0$ represents the auxiliary variables corresponding to (57) and (58), respectively. It can be observed that (59) involves a finite number of LMIs, which thus can be handled using convex optimization techniques.

To tackle constraint (39), we first equivalently transform it into LMIs based on the Schur's complement given by

$$\begin{bmatrix} \beta_{c,k}-\sigma_k^2 & \mathbf{h}_k^H\mathbf{W}_{-k} \\ \mathbf{W}_{-k}^H\mathbf{h}_k & \mathbf{I}_{K-1+N} \end{bmatrix} \succeq \mathbf{0}_{K+N}, \Delta\mathbf{h}_{d,k}\in\mathcal{H}_{d,k}, \Delta\mathbf{F}_k\in\mathcal{F}_k, k\in\mathcal{K}, \quad (60)$$

where $\mathbf{W}_{-k}=[\mathbf{w}_{c,1},\ldots,\mathbf{w}_{c,k-1},\mathbf{w}_{c,k+1},\ldots,\mathbf{w}_{c,K},\mathbf{w}_{r,1},\ldots,\mathbf{w}_{r,N}]$. Substituting $\mathbf{F}_k=\hat{\mathbf{F}}_k+\Delta\mathbf{F}_k$ and $\mathbf{h}_{d,k}=\hat{\mathbf{h}}_{d,k}+\Delta\mathbf{h}_{d,k}$ into (60), this can then be expanded as

$$\begin{aligned} &\begin{bmatrix} \beta_{c,k}-\sigma_k^2 & \left(\mathbf{v}^H\hat{\mathbf{F}}_k+\hat{\mathbf{h}}_{d,k}^H\right)\mathbf{W}_{-k} \\ \mathbf{W}_{-k}^H\left(\hat{\mathbf{F}}_k^H\mathbf{v}+\hat{\mathbf{h}}_{d,k}\right) & \mathbf{I}_{K-1+N} \end{bmatrix} + \begin{bmatrix} \mathbf{0}_{1\times N} \\ \mathbf{W}_{-k}^H \end{bmatrix} \\ &\times\Delta\mathbf{h}_{d,k}\begin{bmatrix} 1 & \mathbf{0}_{1\times(K-1+N)} \end{bmatrix} + \begin{bmatrix} 1 \\ \mathbf{0}_{(K-1+N)\times 1} \end{bmatrix}\Delta\mathbf{h}_{d,k}^H \\ &\times\begin{bmatrix} \mathbf{0}_{N\times 1} & \mathbf{W}_{-k} \end{bmatrix} + \begin{bmatrix} \mathbf{0}_{1\times N} \\ \mathbf{W}_{-k}^H \end{bmatrix}\Delta\mathbf{F}_k^H\begin{bmatrix} \mathbf{v} & \mathbf{0}_{M\times(K-1+N)} \end{bmatrix} \\ &+\begin{bmatrix} \mathbf{v}^H \\ \mathbf{0}_{(K-1+N)\times M} \end{bmatrix}\Delta\mathbf{F}_k\begin{bmatrix} \mathbf{0}_{N\times 1} & \mathbf{W}_{-k} \end{bmatrix} \succeq \mathbf{0}_{K+N}, \\ &\Delta\mathbf{h}_{d,k}\in\mathcal{H}_{d,k}, \Delta\mathbf{F}_k\in\mathcal{F}_k, k\in\mathcal{K}. \end{aligned} \quad (61)$$

To address the infinite number of LMIs in (61), we transform (61) into an equivalent form with only a finite number of LMIs by applying the following lemma:

Lemma 2 (General Sign-Definiteness [49]): Let $\mathbf{Q}\succeq\sum_{i=1}^{\mathrm{I}}\left(\mathbf{A}_i^H\mathbf{X}_i\mathbf{B}_i+\mathbf{B}_i^H\mathbf{X}_i^H\mathbf{A}_i\right)$ and $\|\mathbf{X}_i\|_F\le\varepsilon_i$, where $\mathbf{Q}=\mathbf{Q}^H$. The condition $\{\|\mathbf{X}_i\|_F\le\varepsilon_i\}_{i=1}^{\mathrm{I}}\Rightarrow\mathbf{Q}\succeq\sum_{i=1}^{\mathrm{I}}\left(\mathbf{A}_i^H\mathbf{X}_i\mathbf{B}_i+\mathbf{B}_i^H\mathbf{X}_i^H\mathbf{A}_i\right)$ holds if and only if there exist $\bar{\lambda}_i\ge 0, i\in\{1,\ldots,\mathrm{I}\}$ such that

$$\begin{bmatrix} \mathbf{Q}-\sum_{i=1}^{\mathrm{I}}\bar{\lambda}_i\mathbf{B}_i^H\mathbf{B}_i & -\varepsilon_1\mathbf{A}_1^H & \cdots & -\varepsilon_{\mathrm{I}}\mathbf{A}_{\mathrm{I}}^H \\ -\varepsilon_1\mathbf{A}_1 & \bar{\lambda}_1\mathbf{I} & \cdots & \mathbf{0} \\ \vdots & \vdots & \ddots & \vdots \\ -\varepsilon_{\mathrm{I}}\mathbf{A}_{\mathrm{I}} & \mathbf{0} & \cdots & \bar{\lambda}_{\mathrm{I}}\mathbf{I} \end{bmatrix}\succeq\mathbf{0}. \quad (62)$$

Based on Lemma 2, (61) can be written as (63) (shown at the bottom of the next page), where $\bar{\lambda}_{1,k}\ge 0$ and $\bar{\lambda}_{2,k}\ge 0$ denote the corresponding auxiliary variables. To handle the uncertainty $\Delta\mathbf{F}_r\in\mathcal{F}_r$ in constraint (12c), we introduce auxiliary variables $\{\beta_{r,k}\ge 0\}$ satisfying $\beta_{r,k}=\sum_{i\ne k}^{K}\left|\mathbf{g}^H\mathbf{w}_{c,i}\right|^2+\sum_{n=1}^{N}\left|\mathbf{g}^H\mathbf{w}_{r,n}\right|^2+\sigma_t^2, k\in\mathcal{K}$, and constraint (12c) can be then equivalently transformed as

$$\begin{aligned} &\left|\mathbf{g}^H\mathbf{w}_{c,k}\right|^2\le\beta_{r,k}r_{e,k,\mathrm{th}}, \theta_h\in\Phi_h,\varphi_v\in\Phi_v, \\ &\qquad\Delta\mathbf{F}_r\in\mathcal{F}_r, k\in\mathcal{K}, \end{aligned} \quad (64)$$

$$\begin{aligned} &\sum_{i\ne k}^{K}\left|\mathbf{g}^H\mathbf{w}_{c,i}\right|^2+\sum_{n=1}^{N}\left|\mathbf{g}^H\mathbf{w}_{r,n}\right|^2+\sigma_t^2\ge\beta_{r,k}, \\ &\qquad\theta_h\in\Phi_h,\varphi_v\in\Phi_v,\Delta\mathbf{F}_r\in\mathcal{F}_r,k\in\mathcal{K}. \end{aligned} \quad (65)$$

Similar to the constraint (39), we first transform the inequalities in (64) into LMIs by applying Schur's complement, which yields

$$\begin{bmatrix} \beta_{r,k}r_{e,k,\mathrm{th}} & \mathbf{g}^H\mathbf{w}_{c,k} \\ \mathbf{w}_{c,k}^H\mathbf{g} & 1 \end{bmatrix}\succeq\mathbf{0}_2, \theta_h\in\Phi_h,\varphi_v\in\Phi_v, \Delta\mathbf{F}_r\in\mathcal{F}_r,k\in\mathcal{K}. \quad (66)$$

Recalling that $\mathbf{g}^H=\mathbf{v}^H\mathbf{F}_r$ and substituting $\mathbf{F}_r=\hat{\mathbf{F}}_r+\Delta\mathbf{F}_r$ into (66), the following inequalities are obtained

$$\begin{aligned} &\begin{bmatrix} \beta_{r,k}r_{e,k,\mathrm{th}} & \mathbf{v}^H\hat{\mathbf{F}}_r\mathbf{w}_{c,k} \\ \mathbf{w}_{c,k}^H\hat{\mathbf{F}}_r^H\mathbf{v} & 1 \end{bmatrix} + \begin{bmatrix} \mathbf{v}^H \\ \mathbf{0}_{1\times M} \end{bmatrix}\Delta\mathbf{F}_r\begin{bmatrix} \mathbf{0}_{N\times 1} & \mathbf{w}_{c,k} \end{bmatrix} \\ &+\begin{bmatrix} \mathbf{0}_{1\times N} \\ \mathbf{w}_{c,k}^H \end{bmatrix}\Delta\mathbf{F}_r^H\begin{bmatrix} \mathbf{v} & \mathbf{0}_{M\times 1} \end{bmatrix}\succeq\mathbf{0}_2, \theta_h\in\Phi_h,\varphi_v\in\Phi_v, \\ &\qquad\Delta\mathbf{F}_r\in\mathcal{F}_r. \end{aligned} \quad (67)$$

Based on Lemma 2, constraint (67) involving an infinite number of inequalities can be recast as a finite number of LMIs given by

$$\begin{bmatrix} \beta_{r,k}r_{e,k,\mathrm{th}}-\bar{\lambda}_kM & \mathbf{v}^H\hat{\mathbf{F}}_r\mathbf{w}_{c,k} & \mathbf{0}_{1\times N} \\ \mathbf{w}_{c,k}^H\hat{\mathbf{F}}_r^H\mathbf{v} & 1 & -\varepsilon_r\mathbf{w}_{c,k}^H \\ \mathbf{0}_{N\times 1} & -\varepsilon_r\mathbf{w}_{c,k} & \bar{\lambda}_k\mathbf{I}_N \end{bmatrix}\succeq\mathbf{0}_{N+2}, \theta_h\in\Phi_h,\varphi_v\in\Phi_v,k\in\mathcal{K}, \quad (68)$$

where $\bar{\lambda}_k\ge 0$ represents the corresponding auxiliary variables.

Although constraint (65) is not convex w.r.t $\mathbf{v}$, the left-hand side of (65) is a quadratic function of $\mathbf{v}$. Thus, we can obtain the following lower bound for $\left|\mathbf{g}^H\mathbf{w}_{p,i}\right|^2, p\in\{c,r\}, i\in\mathcal{K}\cup\mathcal{N}$ at any point $\mathbf{v}^r$

$$\begin{aligned} \left|\mathbf{g}^H\mathbf{w}_{p,i}\right|^2\ge&-\left|\mathbf{v}^{r,H}\mathbf{F}_r\mathbf{w}_{p,i}^r\right|^2 \\ &+2\mathrm{Re}\left\{\left(\mathbf{v}^H\mathbf{F}_r\mathbf{w}_{p,i}\right)^H\left(\mathbf{v}^{r,H}\mathbf{F}_r\mathbf{w}_{p,i}^r\right)\right\}. \end{aligned} \quad (69)$$

Substituting $\mathbf{F}_r=\hat{\mathbf{F}}_r+\Delta\mathbf{F}_r$ into $\left|\mathbf{v}^{r,H}\mathbf{F}_r\mathbf{w}_{p,i}^r\right|^2$, we have

$$\begin{aligned} &\left|\mathbf{v}^{r,H}\hat{\mathbf{F}}_r\mathbf{w}_{p,i}^r+\mathbf{v}^{r,H}\Delta\mathbf{F}_r\mathbf{w}_{p,i}^r\right|^2 \\ &=\left|\mathbf{v}^{r,H}\hat{\mathbf{F}}_r\mathbf{w}_{p,i}^r\right|^2 \\ &\quad+\mathrm{vec}^H\left(\Delta\mathbf{F}_r^*\right)\left(\left(\mathbf{w}_{p,i}^r\mathbf{w}_{p,i}^{r,H}\right)^T\otimes\left(\mathbf{v}^r\mathbf{v}^{r,H}\right)\right)^T\mathrm{vec}\left(\Delta\mathbf{F}_r^*\right) \\ &\quad+2\mathrm{Re}\left\{\mathbf{v}^{r,H}\hat{\mathbf{F}}_r\mathbf{w}_{p,i}^r\left(\mathbf{w}_{p,i}^{r,H}\otimes\mathbf{v}^{r,T}\right)\mathrm{vec}\left(\Delta\mathbf{F}_r^*\right)\right\}. \end{aligned} \quad (70)$$

In addition, substituting $\mathbf{F}_r=\hat{\mathbf{F}}_r+\Delta\mathbf{F}_r$ into $\left(\mathbf{v}^H\mathbf{F}_r\mathbf{w}_{p,i}\right)^H\left(\mathbf{v}^{r,H}\mathbf{F}_r\mathbf{w}_{p,i}^r\right)$, we have

$$\begin{aligned} &\left(\mathbf{v}^H\mathbf{F}_r\mathbf{w}_{p,i}\right)^H\left(\mathbf{v}^{r,H}\mathbf{F}_r\mathbf{w}_{p,i}^r\right) \\ &=\mathbf{w}_{p,i}^H\hat{\mathbf{F}}_r^H\mathbf{v}\mathbf{v}^{r,H}\hat{\mathbf{F}}_r\mathbf{w}_{p,i}^r+\mathbf{w}_{p,i}^H\times\hat{\mathbf{F}}_r^H\mathbf{v}\mathrm{vec}^H\left(\Delta\mathbf{F}_r^*\right) \\ &\quad\times\left(\mathbf{w}_{p,i}^r\otimes\mathbf{v}^{r,*}\right)+\mathbf{v}^{r,H}\hat{\mathbf{F}}_r\mathbf{w}_{p,i}^r\left(\mathbf{w}_{p,i}^H\otimes\mathbf{v}^T\right) \\ &\quad\times\mathrm{vec}\left(\Delta\mathbf{F}_r^*\right)+\mathrm{vec}^H\left(\Delta\mathbf{F}_r^*\right)\left(\left(\mathbf{w}_{p,i}^r\mathbf{w}_{p,i}^H\right)\otimes\left(\mathbf{v}^{r,*}\mathbf{v}^T\right)\right) \\ &\qquad\times\mathrm{vec}\left(\Delta\mathbf{F}_r^*\right). \end{aligned} \quad (71)$$

Based on (69), (70), and (71), a lower bound for constraint (65) is given by

$$\mathrm{vec}^H\left(\Delta\mathbf{F}_r^*\right)\mathbf{H}_{\mathrm{temp}}\mathrm{vec}\left(\Delta\mathbf{F}_r^*\right)+\left(\sum_{i\ne k}^{K}c_{c,i}+\sum_{n=1}^{N}c_{r,n}\right)$$

$$+\sigma_t^2+2\mathrm{Re}\left\{\left(\sum_{i\neq k}^{K}\hat{\mathbf{g}}_{c,i}^H+\sum_{n=1}^{N}\hat{\mathbf{g}}_{r,i}^H\right)\mathrm{vec}\left(\Delta\mathbf{F}_r^*\right)\right\}$$
$$\geq \beta_{r,k},\theta_h\in\Phi_h,\varphi_v\in\Phi_v,\Delta\mathbf{F}_r\in\mathcal{F}_r,k\in\mathcal{K}, \quad (72)$$

where $\mathbf{H}_{-k}=\sum_{i\neq k}^{K}\left(\bar{\mathbf{H}}_{c,i}+\bar{\mathbf{H}}_{c,i}^H-\bar{\mathbf{H}}_{c,i}^r\right)+\sum_{n=1}^{N}\left(\bar{\mathbf{H}}_{r,n}+\bar{\mathbf{H}}_{r,n}^H-\bar{\mathbf{H}}_{r,n}^r\right)$, $\bar{\mathbf{H}}_{p,i}=\left(\mathbf{w}_{p,i}^r\mathbf{w}_{p,i}^H\right)\otimes\left(\mathbf{v}^{r,*}\mathbf{v}^T\right)$, $\bar{\mathbf{H}}_{p,i}^r=\left(\mathbf{w}_{p,i}^r\mathbf{w}_{p,i}^{r,H}\right)\otimes\left(\mathbf{v}^r\mathbf{v}^{r,H}\right)^T$, $\hat{\mathbf{g}}_{p,i}^H=\mathbf{v}^H\hat{\mathbf{F}}_r\mathbf{w}_{p,i}\left(\mathbf{w}_{p,i}^{r,H}\otimes\mathbf{v}^{r,T}\right)+\mathbf{v}^{r,H}\hat{\mathbf{F}}_r\mathbf{w}_{p,i}^r\left(\mathbf{w}_{p,i}^H\otimes\mathbf{v}^T\right)-\mathbf{v}^{r,H}\hat{\mathbf{F}}_r\mathbf{w}_{p,i}^r\left(\mathbf{w}_{p,i}^{r,H}\otimes\mathbf{v}^{r,T}\right)$, and $c_{p,i}=2\mathrm{Re}\left\{\mathbf{w}_{p,i}^H\hat{\mathbf{F}}_r^H\mathbf{v}\mathbf{v}^{r,H}\hat{\mathbf{F}}_r\mathbf{w}_{p,i}^r\right\}-\left|\mathbf{v}^{r,H}\hat{\mathbf{F}}_r\mathbf{w}_{p,i}^r\right|^2$. Thus, based on Lemma 1, constraint (72) can be transformed to a finite number of LMIs given by

$$\begin{bmatrix}\mathbf{H}_{-k}+\lambda_{r,k}\mathbf{I}_{MN} & \left(\sum_{i\neq k}^{K}\hat{\mathbf{g}}_{c,i}^H+\sum_{n=1}^{N}\hat{\mathbf{g}}_{r,i}^H\right)^H\\ \sum_{i\neq k}^{K}\hat{\mathbf{g}}_{c,i}^H+\sum_{n=1}^{N}\hat{\mathbf{g}}_{r,i}^H & \left(\sum_{i\neq k}^{K}c_{c,i}+\sum_{n=1}^{N}c_{r,n}\right)+c_{0,k}\end{bmatrix}$$
$$\succeq \mathbf{0}_{MN+1},\theta_h\in\Phi_h,\quad \varphi_v\in\Phi_v,\ k\in\mathcal{K}, \quad (73)$$

where $c_{0,k}=\sigma_t^2-\beta_{r,k}-\lambda_{r,k}\varepsilon_r^2$ and $\lambda_{r,k}\geq 0$ denote the corresponding auxiliary variables.

As a result, problem (12) can be recast as

$$\max_{\{\mathbf{w}_{c,k}\},\{\mathbf{w}_{r,n}\},\{v_m\},\{\beta_{c,k}\},\bar{\lambda},\left\{\bar{\lambda}_{1,k},\bar{\lambda}_{2,k},\lambda_{1,k},\lambda_{2,k},\lambda_{r,k}\right\},\chi}\ \chi \quad (74a)$$
$$\text{s.t. } \mathbf{g}^H\left(\sum_{k=1}^{K}\mathbf{w}_{c,k}\mathbf{w}_{c,k}^H+\sum_{n=1}^{N}\mathbf{w}_{r,n}\mathbf{w}_{r,n}^H\right)\mathbf{g}\geq\chi,\theta_h\in\Phi_h,$$
$$\varphi_v\in\Phi_v,\Delta\mathbf{F}_r\in\mathcal{F}_r, \quad (74b)$$
$$(12d),(12e),(59),(63),(68),(73). \quad (74c)$$

Similarly, by applying Lemma 1, constraint (74b) can be recast as

$$\begin{bmatrix}\bar{\mathbf{H}}_{\mathrm{temp}}+\tilde{\lambda}_r\mathbf{I}_{MN} & \left(\sum_{i=1}^{K}\hat{\mathbf{g}}_{c,i}^H+\sum_{n=1}^{N}\hat{\mathbf{g}}_{r,i}^H\right)^H\\ \sum_{i=1}^{K}\hat{\mathbf{g}}_{c,i}^H+\sum_{n=1}^{N}\hat{\mathbf{g}}_{r,i}^H & \left(\sum_{i\neq k}^{K}c_{c,i}+\sum_{n=1}^{N}c_{r,i}\right)-\chi-\tilde{\lambda}_r\varepsilon_r^2\end{bmatrix}$$
$$\succeq \mathbf{0}_{MN+1},\theta_h\in\Phi_h,\varphi_v\in\Phi_v, \quad (75)$$

where $\bar{\mathbf{H}}_{\mathrm{temp}}=\sum_{i=1}^{K}\left(\bar{\mathbf{H}}_{c,i}+\bar{\mathbf{H}}_{c,i}^H-\bar{\mathbf{H}}_{c,i}^r\right)+\sum_{n=1}^{N}\left(\bar{\mathbf{H}}_{r,n}+\bar{\mathbf{H}}_{r,n}^H-\bar{\mathbf{H}}_{r,n}^r\right)$ and $\tilde{\lambda}_r$ is the auxiliary variable. To solve problem (74), an AO algorithm is proposed to alternatively optimize transformers and IRS phase shifts until convergence is reached. Below, we elaborate on how to solve these two subproblems.

1) Optimizing BS Beamformers With Fixed IRS Phase Shifts: This subproblem is given by

$$\max_{\left\{\mathbf{w}_{c,k},\mathbf{w}_{r,n},\beta_{c,k},\bar{\lambda}_k,\bar{\lambda}_{1,k},\bar{\lambda}_{2,k},\lambda_{1,k},\lambda_{2,k},\lambda_{r,k}\right\},\chi}\ \chi \quad (76a)$$
$$\text{s.t. } (12d),(59),(63),(68),(73),(75). \quad (76b)$$

It can be readily verified that problem (76) is a semi-definite program (SDP), which can be efficiently tackled by standard convex optimization solvers.

2) Optimizing IRS Phase Shifts With Fixed BS Beamformers: This subproblem is written as

$$\max_{\left\{v_m,\beta_{c,k},\bar{\lambda}_k,\bar{\lambda}_{1,k},\bar{\lambda}_{2,k},\lambda_{1,k},\lambda_{2,k},\lambda_{r,k}\right\},\chi}\ \chi \quad (77a)$$
$$\text{s.t. } (12e),(59),(63),(68),(73),(75). \quad (77b)$$

It can be observed that all constraints are convex except (12e) due to the unit-modulus constraint, which is in general difficult to tackle. Fortunately, by applying the square penalty approach [50], problem (77) is equivalent to

$$\max_{\left\{v_m,\beta_{c,k}\bar{\lambda}_k,\bar{\lambda}_{1,k},\bar{\lambda}_{2,k},\lambda_{1,k},\lambda_{2,k},\lambda_{r,k}\right\},\chi}\ \chi+\bar{\rho}\|\mathbf{v}\|^2 \quad (78a)$$
$$\text{s.t. } |v_m|\leq 1,m\in\mathcal{M}, \quad (78b)$$
$$(59),(63),(68),(73),(75), \quad (78c)$$

where $\bar{\rho}$ represents a sufficiently large positive penalty parameter used to make constraint (78b) met with equality at the optimal solution. Note that this equivalence does not require gradually adjusting $\bar{\rho}$ as a large $\bar{\rho}$ suffices. The rigorous proof can be found in [50, Theorem 1] for details. To tackle the non-convex objective function in (78), a lower bound for $\|\mathbf{v}\|^2$ is obtained by applying the SCA. Specifically, for any given $\mathbf{v}^r$, we have

$$\|\mathbf{v}\|^2\geq-\|\mathbf{v}^r\|^2+2\mathrm{Re}\left\{\mathbf{v}^H\mathbf{v}^r\right\}, \quad (79)$$

which is linear w.r.t. $\mathbf{v}$.

As a result, based on (79) and dropping irrelevant terms, problem (78) can be approximated as

$$\max_{\left\{v_m,\beta_{c,k},\bar{\lambda}_k,\bar{\lambda}_{1,k},\bar{\lambda}_{2,k},\lambda_{1,k},\lambda_{2,k},\lambda_{r,k}\right\},\chi}\ \chi+2\bar{\rho}\mathrm{Re}\left\{\mathbf{v}^H\mathbf{v}^r\right\} \quad (80a)$$
$$\text{s.t. } (59),(63),(68),(73),(75),(78b), \quad (80b)$$

which is convex and can be solved by convex optimization solvers.

Finally, we alternately optimize the above two subproblems, and the details are summarized in Algorithm 2. In Algorithm 2, since problems (76) and (80) are convex, which are solved with globally optimal solutions. As such, the objective value of (12) is non-decreasing over iterations. In addition, the maximum objective value of problem

$$\begin{bmatrix}\beta_{c,k}-\sigma_k^2-\bar{\lambda}_{1,k}-\bar{\lambda}_{2,k}M & \left(\mathbf{v}^H\hat{\mathbf{F}}_k+\hat{\mathbf{h}}_{d,k}^H\right)\mathbf{W}_{-k} & \mathbf{0}_{1\times N} & \mathbf{0}_{1\times N}\\ \mathbf{W}_{-k}^H\left(\hat{\mathbf{F}}_k^H\mathbf{v}+\hat{\mathbf{h}}_{d,k}\right) & \mathbf{I}_{K-1+N} & -\varepsilon_{d,k}\mathbf{W}_{-k}^H & -\varepsilon_k\mathbf{W}_{-k}^H\\ \mathbf{0}_{N\times 1} & -\varepsilon_{d,k}\mathbf{W}_{-k} & \bar{\lambda}_{1,k}\mathbf{I}_N & \mathbf{0}_N\\ \mathbf{0}_{N\times 1} & -\varepsilon_k\mathbf{W}_{-k} & \mathbf{0}_N & \bar{\lambda}_{2,k}\mathbf{I}_N\end{bmatrix}\succ\mathbf{0}_{K+3N},\quad k\in\mathcal{K}, \quad (63)$$

Algorithm 2 The AO Algorithm for Solving Problem (12)

1: **Initialize** v_m and ε.
2: **repeat**
3: Update BS beamformers by solving problem (76).
4: Update IRS phase shifts by solving problem (80).
5: **until** the fractional increase of the objective value is less than ε.

(12) is upper-bounded by a finite value due to the limited BS transmit power. As such, Algorithm 2 is guaranteed to converge. Since problems (76) and (80) are SDPs, the total complexity of Algorithm 2 is given by $\mathcal{O}\left(L\left(K\left((N+MN+1)^{6.5}+(K+3N)^{6.5}\right)+\bar{K}(N+2)^{6.5}+\left(\bar{K}+1\right)(MN+1)^{6.5}\right)\right)$, where L stands for the number of iterations required for reaching convergence and $\bar{K}$ denotes the number of LMIs in (68) and (73).

V. Numerical Results

In this section, we provide numerical results to validate the secure transmission performance in the IRS-aided ISAC system. A three dimensional coordinate setup measured in meters (m) is considered, where the BS is located at $(0, 0, 2.5)$ m and the users are uniformly and randomly distributed in a circle of a radius 2 m centered at $(20, 5, 0)$ m, while the IRS is deployed at $(20, 0, 2.5)$ m. The distance-dependent path loss model is given by $L\left(\hat{d}\right) = c_0\left(\hat{d}/d_0\right)^{-\hat{\alpha}}$, where $c_0 = -30$ dB is the path loss at the reference distance $d_0 = 1$ m, $\hat{d}$ is the link distance, and $\hat{\alpha}$ is the path loss exponent. The target is located at azimuth direction $\theta = -30°$ and elevation direction $\varphi = 40°$. We assume that the distance between the IRS and the target is 10 m with a path loss exponent of 2, and assume that the BS-IRS link and the IRS-user link follow Rician fading with a Rician factor of 3 dB and a path loss exponent of 2.2, while the BS-user link follows Rayleigh fading with a path loss exponent of 3.6 due to the assumption of locally rich scattering. The minimum communication SINR and the maximum tolerable intercepting SINR are assumed to be the same for all users, i.e., $r_{c,\text{th}} = r_{k,\text{th}}, r_{e,\text{th}} = r_{e,k,\text{th}}, k \in \mathcal{K}$. Unless otherwise specified, we set $N = 4$, $K = 3$, $\theta = -30°, \varphi = 40°$, $\sigma_k^2 = -90$ dBm, $\forall k$, $\sigma_t^2 = -90$ dBm, $\rho = 0.1$, $c = 0.85$, $\varepsilon_{\text{in}} = 10^{-2}$, and $\varepsilon = \varepsilon_{\text{out}} = 10^{-4}$.

A. Perfect CSI and Known Target Location

In this subsection, we consider the ideal case where the CSI and the target location are known at the BS, and the penalty-based algorithm, i.e., Algorithm 1, is employed.

1) Convergence Behavior of Algorithm 1: We first study the convergence behavior of Algorithm 1 for different numbers of IRS reflecting elements, namely $M = 50$, $M = 100$, and $M = 150$, as shown in Fig. 2. It is observed from Fig. 2(a) that the constraint violation parameter ξ converges very rapidly to a predefined accuracy 10^{-4} after about 75-80 iterations for all values of M. Note that the predefined accuracy value of 10^{-4} is sufficiently small for ensuring that constraint (13d) is essentially met with equality at the optimal solution, since we normalize the channel coefficients by the noise power so that the auxiliary variables are inherently large to guarantee sufficient numerical accuracy. To see it more clearly, we can observe from Fig. 2(b) that the objective value of problem (14) converges quickly for different M, which demonstrates the efficiency of Algorithm 1.

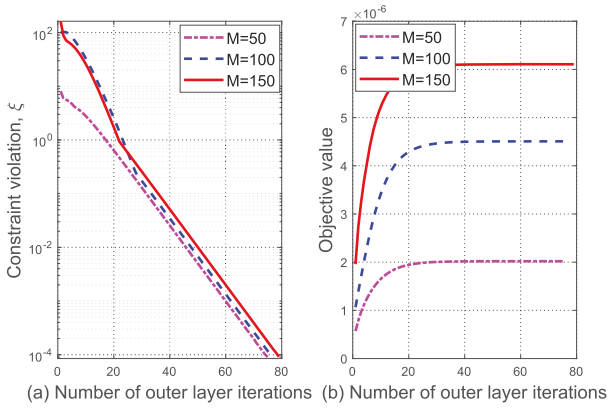

Fig. 2. Convergence behaviour of Algorithm 1 under $P_{\max} = 40$ dBm, $r_{c,\text{th}} = 10$ dB, and $r_{e,\text{th}} = 0$ dB.

To show the superiority of the proposed approach, we consider the following approaches for comparison.

- **Proposed approach:** This is our proposed approach described in Algorithm 1 in Section III.
- **Communication signal only:** Similar to the proposed approach, but without dedicated radar waveforms.
- **Separate beamforming:** This approach optimizes the transmit beamformers and IRS phase shifts separately. The algorithm first obtains the IRS phase-shift matrix by maximizing the norm of the IRS's cascaded channel towards the desired sensing target, i.e, $\max_{\boldsymbol{\Theta}} \left\|\mathbf{g}_r^H \boldsymbol{\Theta} \boldsymbol{G}\right\|$. Then, with the obtained $\boldsymbol{\Theta}$, the transmit beamformers are obtained by solving problem (8).
- **Communication-based zero-forcing (ZF):** The IRS phase-shift matrix is obtained in the same way as the separate beamforming approach, while the communication beamformers, $\mathbf{w}_{c,k}, k \in \mathcal{K}$, are forced to lie in the null space of the target's channel, i.e., $\mathbf{g}^H \mathbf{w}_{c,k} = 0, k \in \mathcal{K}$. The communication covariance matrices are given by $\mathbf{W}_{c,k} = \left(\mathbf{I}_N - \mathbf{g}\mathbf{g}^H/\|\mathbf{g}\|^2\right) \hat{\mathbf{W}}_{c,k} \left(\mathbf{I}_N - \mathbf{g}\mathbf{g}^H/\|\mathbf{g}\|^2\right)^H$, where $\text{rank}\left(\hat{\mathbf{W}}_{c,k}\right) = 1, \hat{\mathbf{W}}_{c,k} \succeq \mathbf{0}_N$. Then, $\hat{\mathbf{W}}_{c,k}$ and the radar covariance matrices are jointly optimized by using the AO algorithm.
- **Sensing-based ZF:** Similar to the communication-based ZF approach, the radar beamformers, i.e., $\mathbf{w}_{r,n}, n \in \mathcal{N}$, are forced to lie in the null space of the users' channels i.e., $\mathbf{h}_k^H \mathbf{w}_{r,n} = 0, k \in \mathcal{K}, n \in \mathcal{N}$. The radar beamformers are designed as $\mathbf{W}_r = \mathbf{V}\hat{\mathbf{W}}_r$, where $\mathbf{V}$ represents the

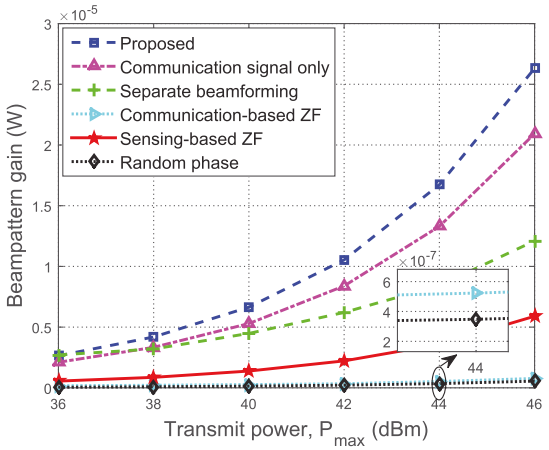

Fig. 3. Beampattern gain versus $P_{\max}$ under $M = 100$, $r_{c,\text{th}} = 10$ dB, and $r_{e,\text{th}} = 0$ dB.

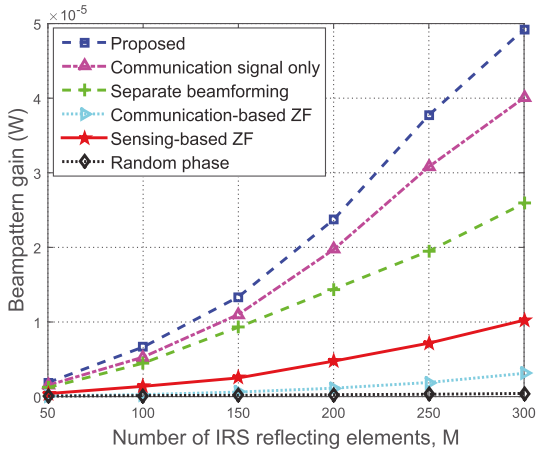

Fig. 4. Beampattern gain versus M under $P_{\max} = 40$ dBm, $r_{c,\text{th}} = 10$ dB, and $r_{e,\text{th}} = 0$ dB.

last $N-K$ right singular vectors of $\mathbf{H} = [\mathbf{h}_1, \ldots, \mathbf{h}_K]^H$. Then, the communication beamformers and $\hat{\mathbf{W}}_r$ are jointly optimized by using the penalty-based algorithm.

- **Random phase:** The IRS phase shifts are generated randomly following a uniform distribution over $[0, 2\pi)$.

2) Beampattern Gain Versus Transmit Power: In Fig. 3, we compare the beampattern gain of the above approaches versus $P_{\max}$. We see that the beampattern gain for all methods increases monotonically with $P_{\max}$ since the co-channel interference is suppressed and increasing the available power improves the beampattern gain. In addition, we observe that the proposed approach outperforms the "Communication signal only" case, which indicates the benefit of dedicated radar signals. This can be explained as follows. The additional radar signals provide more DoFs for algorithm optimization, which improves the system performance, and to prevent the eavesdropping by the target, more power must be allocated to the radar signals and the beampattern gain is thus increased. Moreover, we observe that the beampattern gain obtained by the approaches without IRS phase shift optimization increases marginally as $P_{\max}$ increases since the signals reflected by the IRS in this case are propagated in many random directions, thus results in a low received power level. Furthermore, compared to the "Separate beamforming", "Communication-based ZF", and "Sensing-based ZF" approaches, our proposed approach achieves significant beampattern gains, which illustrates the benefit of joint design of the transmit beamformers and IRS phase shifts.

3) Beampattern Gain Versus Number of IRS Reflecting Elements: In Fig. 4, we compare the beampattern gain for all approaches versus M. It is observed that the proposed approach outperforms the "Random phase" approach, and the system performance gap is more pronounced for a larger M. This is because installing more passive reflecting elements provides more DoFs for resource allocation, which is beneficial for achieving higher beamforming gain, thereby improving the beampattern gain when the IRS phase shifts are well adjusted. In addition, we again observe that our proposed approach outperforms the use of only communication signals, further amplifying the benefit of using dedicated radar signals. Moreover, the performance gap between our proposed approach and the "Separate beamforming", "Communication-based ZF", and "Sensing-based ZF" approaches is magnified as M increases, which again demonstrates the benefit of joint design of the transmit beamformers and IRS phase shifts.

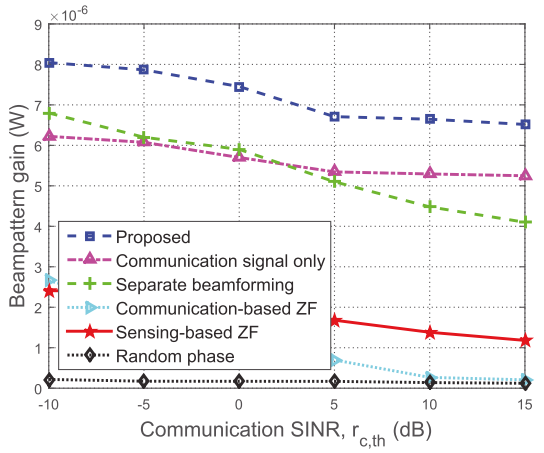

Fig. 5. Beampattern gain versus $r_{c,\text{th}}$ under $M = 100$, $P_{\max} = 40$ dBm, and $r_{e,\text{th}} = 0$ dB.

4) Beampattern Gain Versus Minimum SINR Required by Communication Users: In Fig. 5, the achieved beampattern gain is plotted versus the communication users' SINR requirement $r_{c,\text{th}}$. As expected, a more stringent QoS requirement for the users results in a lower beamforming gain to the target, since the BS and IRS must focus more energy towards the communication users. In addition, we observe that the performance gap between our proposed approach and the "Separate beamforming" approach becomes smaller as $r_{c,\text{th}}$ decreases. This is because in this case the SINR at the users can be easily satisfied, and thus extra radar and communication power can be used to improve the beampatter gain. Moreover, we observe that the performance of the "Communication-based ZF" approach degrades quickly as $r_{c,\text{th}}$ increases. This is because communication signals are forced to lie in the null space of target's channel, which indicates that no user information is leaked to the target and only the radar signals

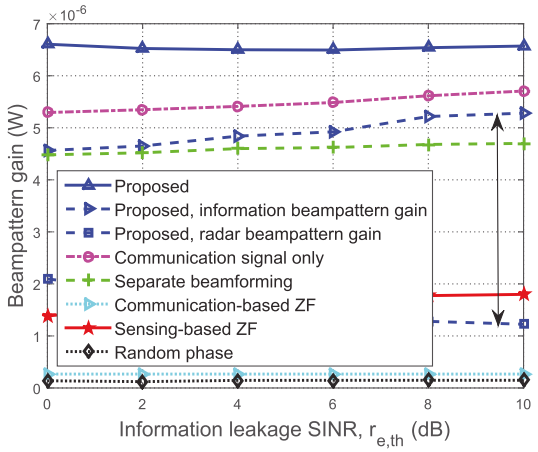

Fig. 6. Beampattern gain versus $r_{e,\mathrm{th}}$ under $M = 100$, $P_{\max} = 40$ dBm, and $r_{c,\mathrm{th}} = 10$ dB.

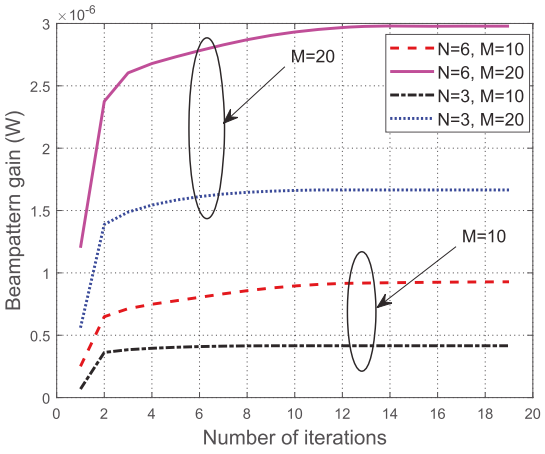

Fig. 7. Convergence behaviour of Algorithm 2 for different M and N.

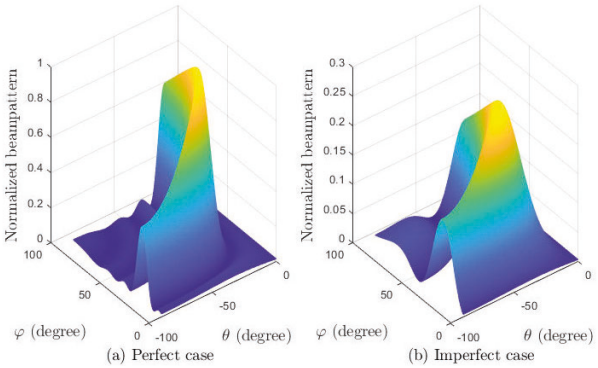

Fig. 8. Three-dimensional (3D) Beampattern design for different system setups.

can be used to increase the beampattern gain. On the other hand, increasing the radar power potentially degrades the user SINR, which limits the improvement of beampattern gain.

5) Beampattern Gain Versus Maximum Information Leakage SINR to Target: We further study the beampattern gain versus the leakage constraint $r_{e,\mathrm{th}}$ in Fig. 6. Interestingly, we observe that the beampattern gain obtained by the proposed approach remains nearly unchanged with $r_{e,\mathrm{th}}$. To unveil the reason behind this, the separate radar and communication power contributions to the beampattern gain versus $r_{e,\mathrm{th}}$ are studied, i.e., $\sum_{n=1}^{N}\left|\mathbf{w}_{r,n}^{H}\mathbf{g}\right|^2$ and $\sum_{k=1}^{K}\left|\mathbf{w}_{c,k}^{H}\mathbf{g}\right|^2$, which correspond to the "Proposed, radar beampattern gain" and the "Proposed, information beampattern gain" approaches, respectively. We see that as the requirement on signal leakage to the target is made less stringent (i.e., $r_{e,\mathrm{th}}$ increases), less transmit power is allocated to radar signals to deteriorate the reception by the eavesdropping target, while more power is allocated to the information signals to improve the communication QoS. In the end, these two trends offset each other, and the sum of the two components results in a nearly constant beampattern gain. In addition, we observe that the performance gain obtained by the "Sensing-based ZF" approach increases marginally as $r_{e,\mathrm{th}}$ increases due to the limited DoFs available for design of the radar beamformers.

B. Imperfect CSI and Uncertain Target Location

In this subsection, we consider the case with imperfect CSI and unknown potential target location in a region of interest, and we propose Algorithm 2 to address the resulting problem. The azimuth and elevation target location ranges are set to $\Phi_h = [-35°, -25°]$ and $\Phi_v = [35°, 45°]$, respectively. We define the relative amount of CSI errors as $\hat{\varepsilon}_r = \varepsilon_r / \left\|\hat{\mathbf{F}}_r\right\|_F$, $\hat{\varepsilon}_k = \varepsilon_k / \left\|\hat{\mathbf{F}}_k\right\|_F$, and $\hat{\varepsilon}_{d,k} = \varepsilon_{d,k} / \left\|\hat{\mathbf{h}}_{d,k}\right\|, \forall k$, respectively. For ease of exposition, we assume that all channels have the same level of CSI errors, i.e., $\varepsilon_{\mathrm{error}} = \hat{\varepsilon}_r = \hat{\varepsilon}_k = \hat{\varepsilon}_{d,k}, \forall k$.

1) Convergence Behavior of Algorithm 2: In Fig. 7, the convergence behaviour of Algorithm 2 for different M and N under $\varepsilon_{\mathrm{error}} = 0.01$, $P_{\max} = 46$ dBm, $K = 2$, $r_{c,\mathrm{th}} = 10$ dB, and $r_{e,\mathrm{th}} = 5$ dB is studied. It is observed that the obtained beampattern gain is monotonically increasing with the number of iterations and ultimately converges. Even for $M = 20$ and $N = 6$, the proposed algorithm converges in about 20 iterations, which demonstrates the effectiveness of Algorithm 2.

2) Beampattern Design: In Fig. 8, we study the normalized 3D beampattern obtained in the case with perfect CSI and the known target location and with the case of imperfect CSI and uncertain target location when $M = 20$, $N = 3$, $\varepsilon_{\mathrm{error}} = 0.01$, $P_{\max} = 46$ dBm, $K = 2$, $r_{c,\mathrm{th}} = 10$ dB, and $r_{e,\mathrm{th}} = 5$ dB. Both beampatterns are normalized by the maximum value of these two beampatterns. It is observed that both of the beampatterns obtained by our proposed algorithms correctly focus their mainlobe towards the directions $\theta = -30°$ and $\varphi = 40°$. In addition, we observe that both beampatterns have sidelobe regions due to the imposed SINR constraints for the users as well as the information leakage to the eavesdropping target. Furthermore, we observe that the mainlobe in the imperfect CSI case is more flatter and wider than that with perfect CSI case. This is expected since although the exact target location is unknown, its range of possible locations is known, so that the probing power should uniformly cover this area rather than focusing on a point in one direction. Moreover, we observe that the peak beampattern gain of the imperfect CSI case is lower than with in the perfect CSI case due to the reduced available information.

3) Beampattern Gain Versus M: In Fig. 9, we study the beampattern gain versus M for different N and $\varepsilon_{\mathrm{error}}$ under

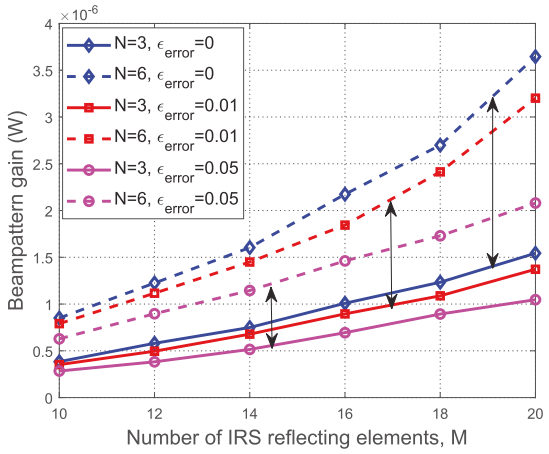

Fig. 9. Beampattern gain versus M for different N and $\varepsilon_{\text{error}}$.

$P_{\max} = 46$ dBm, $K = 2$, $r_{e,\text{th}} = 5$ dB, and $r_{c,\text{th}} = 10$ dB. A large $\varepsilon_{\text{error}}$ indicates that the channel estimation error is magnified and $\varepsilon_{\text{error}} = 0$ corresponds to the perfect CSI case. It is observed that the beampattern gain obtained by different N and $\varepsilon_{\text{error}}$ monotonically increases with M. This observation shows that by carefully designing the BS beamformers and the IRS phase shifts, the system performance can still be improved with imperfect CSI even with large channel estimation errors, e.g., $\varepsilon_{\text{error}} = 0.05$. Furthermore, we observe that for a fixed M, the beampattern gain increases with N. This is due to the fact that more DoFs can be exploited for resource allocation to achieve higher array gain.

VI. Conclusion

In this paper, we proposed the use of IRS to achieve simultaneous secure communication and sensing in the presence of an eavesdropping target and multiple communication users. The communication beamformers, the radar beamformers, and the IRS phase shifts were jointly optimized to maximize the sensing beampattern gain while satisfying the minimum SINR required by the users and secrecy constraint for the eavesdropping target. For the first scenario where the CSI of the user links and the target location are known, a penalty-based algorithm was proposed to solve the formulated non-convex optimization problem. In particular, the beamformers were obtained via a semi-closed-form solution using the Lagrange duality method and the IRS phase shifts were obtained in closed-form by applying the MM method. For the second scenario where the CSI and the target location are imprecisely unknown, an efficient AO algorithm based on the $\mathcal{S}$-procedure and sign-definiteness approaches was proposed. Simulation results verified the effectiveness of the proposed scheme in achieving a flexible trade-off between the communication quality and the target sensing quality and showed the capability of the IRS for use in sensing and improving the physical layer security of ISAC systems. In addition, the simulation results also illustrated the benefits of using dedicated sensing signals to improve the sensing quality.

References

[1] A. Liu et al., "A survey on fundamental limits of integrated sensing and communication," *IEEE Commun. Surveys Tuts.*, vol. 24, no. 2, pp. 994–1034, 2nd Quart., 2022.

[2] L. Zheng, M. Lops, Y. C. Eldar, and X. Wang, "Radar and communication coexistence: An overview: A review of recent methods," *IEEE Signal Process. Mag.*, vol. 36, no. 5, pp. 85–99, Sep. 2019.

[3] F. Liu et al., "Integrated sensing and communications: Toward dual-functional wireless networks for 6G and beyond," *IEEE J. Sel. Areas Commun.*, vol. 40, no. 6, pp. 1728–1767, Jun. 2022.

[4] J. A. Zhang et al., "Enabling joint communication and radar sensing in mobile networks—A survey," *IEEE Commun. Surveys Tuts.*, vol. 24, no. 1, pp. 306–345, 1st Quart., 2022.

[5] Y. Cui, F. Liu, X. Jing, and J. Mu, "Integrating sensing and communications for ubiquitous IoT: Applications, trends, and challenges," *IEEE Netw.*, vol. 35, no. 5, pp. 158–167, Sep. 2021.

[6] C. Sturm and W. Wiesbeck, "Waveform design and signal processing aspects for fusion of wireless communications and radar sensing," *Proc. IEEE*, vol. 99, no. 7, pp. 1236–1259, Jul. 2011.

[7] A. Hassanien, M. G. Amin, Y. D. Zhang, and F. Ahmad, "Dual-function radar-communications: Information embedding using sidelobe control and waveform diversity," *IEEE Trans. Signal Process.*, vol. 64, no. 8, pp. 2168–2181, Apr. 2016.

[8] X. Liu, T. Huang, N. Shlezinger, Y. Liu, J. Zhou, and Y. C. Eldar, "Joint transmit beamforming for multiuser MIMO communications and MIMO radar," *IEEE Trans. Signal Process.*, vol. 68, pp. 3929–3944, 2020.

[9] F. Liu, L. Zhou, C. Masouros, A. Li, W. Luo, and A. Petropulu, "Toward dual-functional radar-communication systems: Optimal waveform design," *IEEE Trans. Signal Process.*, vol. 66, no. 16, pp. 4264–4279, Aug. 2018.

[10] H. Hua, J. Xu, and T. X. Han, "Optimal transmit beamforming for integrated sensing and communication," *IEEE Trans. Veh. Technol.*, early access, Mar. 29, 2023, doi: 10.1109/TVT.2023.3262513.

[11] K. Meng, Q. Wu, S. Ma, W. Chen, K. Wang, and J. Li, "Throughput maximization for UAV-enabled integrated periodic sensing and communication," *IEEE Trans. Wireless Commun.*, vol. 22, no. 1, pp. 671–687, Jan. 2023.

[12] Z. Lyu, G. Zhu, and J. Xu, "Joint maneuver and beamforming design for UAV-enabled integrated sensing and communication," *IEEE Trans. Wireless Commun.*, vol. 22, no. 4, pp. 2424–2440, Apr. 2023.

[13] K. Meng, Q. Wu, S. Ma, W. Chen, and T. Q. S. Quek, "UAV trajectory and beamforming optimization for integrated periodic sensing and communication," *IEEE Wireless Commun. Lett.*, vol. 11, no. 6, pp. 1211–1215, Jun. 2022.

[14] Q. Wu et al., "A comprehensive overview on 5G-and-beyond networks with UAVs: From communications to sensing and intelligence," *IEEE J. Sel. Areas Commun.*, vol. 39, no. 10, pp. 2912–2945, Oct. 2021.

[15] Q. Wu and R. Zhang, "Towards smart and reconfigurable environment: Intelligent reflecting surface aided wireless network," *IEEE Commun. Mag.*, vol. 58, no. 1, pp. 106–112, Jan. 2020.

[16] C. Pan et al., "An overview of signal processing techniques for RIS/IRS-aided wireless systems," *IEEE J. Sel. Topics Signal Process.*, vol. 16, no. 5, pp. 883–917, Aug. 2022.

[17] Q. Wu and R. Zhang, "Beamforming optimization for wireless network aided by intelligent reflecting surface with discrete phase shifts," *IEEE Trans. Commun.*, vol. 68, no. 3, pp. 1838–1851, Mar. 2020.

[18] G. Chen, Q. Wu, W. Chen, D. W. K. Ng, and L. Hanzo, "IRS-aided wireless powered MEC systems: TDMA or NOMA for computation offloading?" *IEEE Trans. Wireless Commun.*, vol. 22, no. 2, pp. 1201–1218, Feb. 2023.

[19] T. Bai, C. Pan, Y. Deng, M. Elkashlan, A. Nallanathan, and L. Hanzo, "Latency minimization for intelligent reflecting surface aided mobile edge computing," *IEEE J. Sel. Areas Commun.*, vol. 38, no. 11, pp. 2666–2682, Nov. 2020.

[20] G. Chen, Q. Wu, C. He, W. Chen, J. Tang, and S. Jin, "Active IRS aided multiple access for energy-constrained IoT systems," *IEEE Trans. Wireless Commun.*, vol. 22, no. 3, pp. 1677–1694, Mar. 2023.

[21] Q. Wu and R. Zhang, "Joint active and passive beamforming optimization for intelligent reflecting surface assisted SWIPT under QoS constraints," *IEEE J. Sel. Areas Commun.*, vol. 38, no. 8, pp. 1735–1748, Aug. 2020.

[22] Z. Chu, P. Xiao, D. Mi, W. Hao, M. Khalily, and L. Yang, "A novel transmission policy for intelligent reflecting surface assisted wireless powered sensor networks," *IEEE J. Sel. Topics Signal Process.*, vol. 15, no. 5, pp. 1143–1158, Aug. 2021.

[23] Q. Wu, X. Zhou, and R. Schober, "IRS-assisted wireless powered NOMA: Do we really need different phase shifts in DL and UL?" *IEEE Wireless Commun. Lett.*, vol. 10, no. 7, pp. 1493–1497, Jul. 2021.

[24] M. Hua and Q. Wu, "Joint dynamic passive beamforming and resource allocation for IRS-aided full-duplex WPCN," *IEEE Trans. Wireless Commun.*, vol. 21, no. 7, pp. 4829–4843, Jul. 2022.
[25] C. Pan et al., "Multicell MIMO communications relying on intelligent reflecting surfaces," *IEEE Trans. Wireless Commun.*, vol. 19, no. 8, pp. 5218–5233, Aug. 2020.
[26] H. Xie, J. Xu, and Y. Liu, "Max-min fairness in IRS-aided multi-cell MISO systems with joint transmit and reflective beamforming," *IEEE Trans. Wireless Commun.*, vol. 20, no. 2, pp. 1379–1393, Feb. 2021.
[27] M. Hua, Q. Wu, D. W. K. Ng, J. Zhao, and L. Yang, "Intelligent reflecting surface-aided joint processing coordinated multipoint transmission," *IEEE Trans. Commun.*, vol. 69, no. 3, pp. 1650–1665, Mar. 2021.
[28] R. Liu, M. Li, H. Luo, Q. Liu, and A. L. Swindlehurst, "Integrated sensing and communication with reconfigurable intelligent surfaces: Opportunities, applications, and future directions," *IEEE Wireless Commun.*, vol. 30, no. 1, pp. 50–57, Feb. 2023.
[29] S. Buzzi, E. Grossi, M. Lops, and L. Venturino, "Foundations of MIMO radar detection aided by reconfigurable intelligent surfaces," *IEEE Trans. Signal Process.*, vol. 70, pp. 1749–1763, 2022.
[30] W. Lu, Q. Lin, N. Song, Q. Fang, X. Hua, and B. Deng, "Target detection in intelligent reflecting surface aided distributed MIMO radar systems," *IEEE Sensors Lett.*, vol. 5, no. 3, pp. 1–4, Mar. 2021.
[31] X. Shao, C. You, W. Ma, X. Chen, and R. Zhang, "Target sensing with intelligent reflecting surface: Architecture and performance," *IEEE J. Sel. Areas Commun.*, vol. 40, no. 7, pp. 2070–2084, Jul. 2022.
[32] Z. Jiang et al., "Intelligent reflecting surface aided dual-function radar and communication system," *IEEE Syst. J.*, vol. 16, no. 1, pp. 475–486, Mar. 2022.
[33] X. Song, D. Zhao, H. Hua, T. X. Han, X. Yang, and J. Xu, "Joint transmit and reflective beamforming for IRS-assisted integrated sensing and communication," in *Proc. IEEE WCNC*, Austin, TX, USA, Apr. 2022, pp. 189–194.
[34] X. Wang, Z. Fei, Z. Zheng, and J. Guo, "Joint waveform design and passive beamforming for RIS-assisted dual-functional radar-communication system," *IEEE Trans. Veh. Technol.*, vol. 70, no. 5, pp. 5131–5136, May 2021.
[35] R. Liu, M. Li, Y. Liu, Q. Wu, and Q. Liu, "Joint transmit waveform and passive beamforming design for RIS-aided DFRC systems," *IEEE J. Sel. Topics Signal Process.*, vol. 16, no. 5, pp. 995–1010, Aug. 2022.
[36] R. Sankar and S. P. Chepuri, "Beamforming in hybrid RIS assisted integrated sensing and communication systems," in *Proc. EUSIPCO*, Belgrade, Serbia, 2022, pp. 1082–1086.
[37] N. Su, F. Liu, and C. Masouros, "Secure radar-communication systems with malicious targets: Integrating radar, communications and jamming functionalities," *IEEE Trans. Wireless Commun.*, vol. 20, no. 1, pp. 83–95, Jan. 2021.
[38] N. Su, F. Liu, Z. Wei, Y. Liu, and C. Masouros, "Secure dual-functional radar-communication transmission: Exploiting interference for resilience against target eavesdropping," *IEEE Trans. Wireless Commun.*, vol. 21, no. 9, pp. 7238–7252, Sep. 2022.
[39] Q. Wu, S. Zhang, B. Zheng, C. You, and R. Zhang, "Intelligent reflecting surface-aided wireless communications: A tutorial," *IEEE Trans. Commun.*, vol. 69, no. 5, pp. 3313–3351, May 2021.
[40] A. Elzanaty, A. Guerra, F. Guidi, and M. Alouini, "Reconfigurable intelligent surfaces for localization: Position and orientation error bounds," *IEEE Trans. Signal Process.*, vol. 69, pp. 5386–5402, 2021.
[41] F. Liu, C. Masouros, A. Li, H. Sun, and L. Hanzo, "MU-MIMO communications with MIMO radar: From co-existence to joint transmission," *IEEE Trans. Wireless Commun.*, vol. 17, no. 4, pp. 2755–2770, Apr. 2018.
[42] C. Hu, L. Dai, S. Han, and X. Wang, "Two-timescale channel estimation for reconfigurable intelligent surface aided wireless communications," *IEEE Trans. Commun.*, vol. 69, no. 11, pp. 7736–7747, Nov. 2021.
[43] X. Yu, D. Xu, Y. Sun, D. W. K. Ng, and R. Schober, "Robust and secure wireless communications via intelligent reflecting surfaces," *IEEE J. Sel. Areas Commun.*, vol. 38, no. 11, pp. 2637–2652, Nov. 2020.
[44] G. Zhou, C. Pan, H. Ren, K. Wang, and A. Nallanathan, "A framework of robust transmission design for IRS-aided MISO communications with imperfect cascaded channels," *IEEE Trans. Signal Process.*, vol. 68, pp. 5092–5106, 2020.
[45] S. Boyd and L. Vandenberghe, *Convex Optimization*. Cambridge, U.K.: Cambridge Univ. Press, 2004.
[46] Y. Sun, P. Babu, and D. P. Palomar, "Majorization-minimization algorithms in signal processing, communications, and machine learning," *IEEE Trans. Signal Process.*, vol. 65, no. 3, pp. 794–816, Feb. 2017.
[47] Q. Shi, M. Hong, X. Gao, E. Song, Y. Cai, and W. Xu, "Joint source-relay design for full-duplex MIMO AF relay systems," *IEEE Trans. Signal Process.*, vol. 64, no. 23, pp. 6118–6131, Dec. 2016.
[48] S. Boyd, L. El Ghaoui, E. Feron, and V. Balakrishnan, *Linear Matrix Inequalities in System and Control Theory*. Philadelphia, PA, USA: SIAM, 1994.
[49] E. A. Gharavol and E. G. Larsson, "The sign-definiteness lemma and its applications to robust transceiver optimization for multiuser MIMO systems," *IEEE Trans. Signal Process.*, vol. 61, no. 2, pp. 238–252, Jan. 2013.
[50] M. Shao, Q. Li, W. Ma, and A. M. So, "A framework for one-bit and constant-envelope precoding over multiuser massive MISO channels," *IEEE Trans. Signal Process.*, vol. 67, no. 20, pp. 5309–5324, Oct. 2019.

Meng Hua (Member, IEEE) received the M.S. degree in electrical and information engineering from the Nanjing University of Science and Technology, Nanjing, China, in 2016, and the Ph.D. degree from the School of Information Science and Engineering, Southeast University, Nanjing, in 2021. He is currently a Post-Doctoral Researcher with the State Key Laboratory of Internet of Things for Smart City, University of Macau. His current research interests include localization, integrated sensing and communication, and intelligent reflecting surface. He was a recipient of the Outstanding Ph.D. Thesis Award from the Chinese Institute of Electronics in 2021.

Qingqing Wu (Senior Member, IEEE) received the B.Eng. degree in electronic engineering from the South China University of Technology in 2012 and the Ph.D. degree in electronic engineering from Shanghai Jiao Tong University (SJTU) in 2016.

From 2016 to 2020, he was a Research Fellow with the Department of Electrical and Computer Engineering, National University of Singapore. He is currently an Associate Professor with Shanghai Jiao Tong University. He has coauthored more than 100 IEEE journal articles with 29 ESI highly cited papers and nine ESI hot papers, which have received more than 19,000 Google citations. He was listed as the Clarivate ESI Highly Cited Researcher in 2022 and 2021 and World's Top 2% Scientist by Stanford University in 2020 and 2021. His current research interests include intelligent reflecting surface (IRS), unmanned aerial vehicle (UAV) communications, and MIMO transceiver design. He received the Most Influential Scholar Award in AI-2000 by Aminer in 2021. He was a recipient of the IEEE Communications Society Asia–Pacific Best Young Researcher Award and the Outstanding Paper Award in 2022, the IEEE Communications Society Young Author Best Paper Award in 2021, the Outstanding Ph.D. Thesis Award from the China Institute of Communications in 2017, the Outstanding Ph.D. Thesis Funding from SJTU in 2016, the IEEE ICCC Best Paper Award in 2021, and IEEE WCSP Best Paper Award in 2015. He is the Workshop Co-Chair of IEEE ICC 2019–2022 Workshop on Integrating UAVs into 5G and Beyond, and IEEE GLOBECOM 2020 and ICC 2021 Workshop on Reconfigurable Intelligent Surfaces for Wireless Communication for Beyond 5G. He serves as the Workshops and Symposia Officer of Reconfigurable Intelligent Surfaces Emerging Technology Initiative and Research Blog Officer of Aerial Communications Emerging Technology Initiative. He is the IEEE Communications Society Young Professional Chair in Asia–Pacific Region. He was an Exemplary Editor of IEEE COMMUNICATIONS LETTERS in 2019 and an exemplary reviewer of several IEEE journals. He serves as an Associate Editor for IEEE TRANSACTIONS ON COMMUNICATIONS, IEEE COMMUNICATIONS LETTERS, IEEE WIRELESS COMMUNICATIONS LETTERS, IEEE OPEN JOURNAL OF COMMUNICATIONS SOCIETY (OJ-COMS), and IEEE OPEN JOURNAL OF VEHICULAR TECHNOLOGY (OJVT). He is the Lead Guest Editor of the IEEE JOURNAL ON SELECTED AREAS IN COMMUNICATIONS on UAV Communications in 5G and Beyond Networks, and the Guest Editor of IEEE OJVT on 6G Intelligent Communications and IEEE OJ-COMS on Reconfigurable Intelligent Surface-Based Communications for 6G Wireless Networks.

Wen Chen (Senior Member, IEEE) is currently a tenured Professor with the Department of Electronic Engineering, Shanghai Jiao Tong University, China, where he is also the Director of the Broadband Access Network Laboratory. He has published more than 130 papers in IEEE journals and more than 120 papers in IEEE Conferences, with citations more than 9000 in Google scholar. His research interests include multiple access, wireless AI, and meta-surface communications. He is a fellow of the Chinese Institute of Electronics. He is an Editor of IEEE TRANSACTIONS ON WIRELESS COMMUNICATIONS, IEEE TRANSACTIONS ON COMMUNICATIONS, IEEE ACCESS, and IEEE OPEN JOURNAL OF VEHICULAR TECHNOLOGY. He is also a Distinguished Lecturer of the IEEE Communications Society and IEEE Vehicular Technology Society. He is the Shanghai Chapter Chair of IEEE Vehicular Technology Society.

Octavia A. Dobre (Fellow, IEEE) received the Dipl.Ing. and Ph.D. degrees from the Polytechnic Institute of Bucharest, Romania, in 1991 and 2000, respectively. From 2002 to 2005, she was with the New Jersey Institute of Technology, USA. In 2005, she joined Memorial University, Canada, where she is currently a Professor and the Canada Research Chair Tier 1. She was a Visiting Professor with the Massachusetts Institute of Technology, USA, and Université de Bretagne Occidentale, France. Her research interests include wireless communication and networking technologies, as well as optical and underwater communications. She has coauthored over 450 refereed papers in these areas. She is an Elected Member of the European Academy of Sciences and Arts and a fellow of the Engineering Institute of Canada and the Canadian Academy of Engineering. She received the Best Paper Awards at various conferences, including IEEE ICC, IEEE Globecom, IEEE WCNC, and IEEE PIMRC. She serves as the Director of Journals of the Communications Society. She was the inaugural Editor-in-Chief (EiC) of the IEEE OPEN JOURNAL OF THE COMMUNICATIONS SOCIETY and the EiC of the IEEE COMMUNICATIONS LETTERS. She served as the general chair, the technical program co-chair, the tutorial co-chair, and the technical co-chair of symposia at numerous conferences. She was a Fulbright Scholar, a Royal Society Scholar, and a Distinguished Lecturer of the IEEE Communications Society.

A. Lee Swindlehurst (Fellow, IEEE) received the B.S. and M.S. degrees in electrical engineering from Brigham Young University (BYU), Provo, UT, USA, in 1985 and 1986, respectively, and the Ph.D. degree in electrical engineering from Stanford University, Stanford, CA, USA, in 1991. He was with the Department of Electrical and Computer Engineering, BYU, from 1990 to 2007. From 1996 to 1997, he held a joint appointment as a Visiting Scholar with Uppsala University, Uppsala, Sweden; and the Royal Institute of Technology, Stockholm, Sweden. From 2006 to 2007, he was on leave working as the Vice President of Research for ArrayComm LLC, San Jose, CA, USA. Since 2007, he has been a Professor with the Department of Electrical Engineering and Computer Science, University of California at Irvine, Irvine, CA, USA. From 2014 to 2017, he was also a Hans Fischer Senior Fellow with the Institute for Advanced Studies, Technical University of Munich, Munich, Germany. His research interests include array signal processing for radar, wireless communications, and biomedical applications, and has more than 400 publications in these areas. In 2016, he was elected as a Foreign Member of the Royal Swedish Academy of Engineering Sciences (IVA). He was a recipient of the 2000 IEEE W. R. G. Baker Prize Paper Award; the 2006 IEEE Communications Society Stephen O. Rice Prize in the Field of Communication Theory; the 2006, 2010, and 2021 IEEE Signal Processing Society Best Paper Awards; the 2017 IEEE Signal Processing Society Donald G. Fink Overview Paper Award; and the Best Paper award at the 2020 IEEE International Conference on Communications. He was the Inaugural Editor-in-Chief of the IEEE JOURNAL OF SELECTED TOPICS IN SIGNAL PROCESSING.